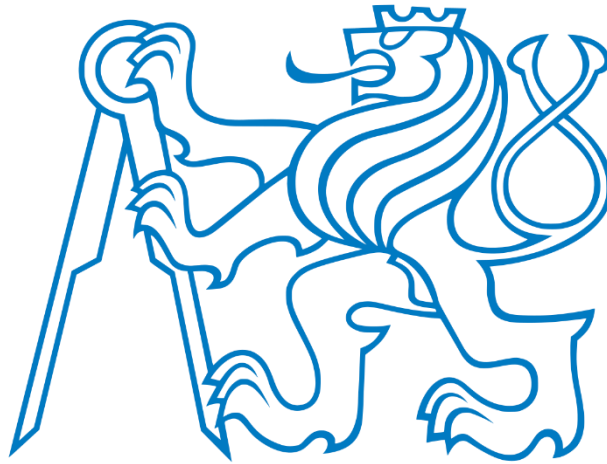




CZECH TECHNICAL UNIVERSITY IN PRAGUE

Faculty of Mechanical Engineering

U12120 - Department of Automotive, Combustion Engine and
Railway Engineering



Diploma thesis

Gearshift simulation model of a dog clutch

Prague

2019

Submitted by: Vijay Jeyaraman

Supervisor: Ing Michal Jasný



MASTER'S THESIS ASSIGNMENT

I. Personal and study details

Student's name: Jeyaraman Vijay Personal ID number: 465797
Faculty / Institute: Faculty of Mechanical Engineering
Department / Institute: Department of Automotive, Combustion Engine and Railway Engineering
Study program: Master of Automotive Engineering
Branch of study: Advanced Powertrains

II. Master's thesis details

Master's thesis title in English:

Gearshift Simulation Model of a Dog Clutch

Master's thesis title in Czech:

Simulační model řazení čelní zubové spojky

Guidelines:

Choose an appropriate simulation software for a gearshift simulation model of face dog clutch engagement (e.g. Simpack, Adams...).

Create a gearshift simulation model of face dog clutch engagement with attention to the dog's geometry (especially number of dogs, their shape).

Use one of the existing dog clutch prototypes to compare the simulation model with experimental gearshifts carried out at the inertia testing bench at Juliska.

Bibliography / sources:

NAUNHEIMER, H., BERTSCH, B., RYBORZ, J., NOVAK, W. Automotive Transmissions. Fundamentals, Selection, Design and Application. Berlin : Springer-Verlag, 2011. ISBN 978-3-642-16216-8.

BÓKA, Gergely. Shifting Optimization of Face Dog Clutches in Heavy Duty Automated Mechanical Transmissions. Budapest : Budapest University of Technology and Economics, 2011. Dissertation thesis.

Name and workplace of master's thesis supervisor:

Ing. Michal Jasný, Department of Automotive, Combustion Engine and Railway Engineering, FME

Name and workplace of second master's thesis supervisor or consultant:

Date of master's thesis assignment: 18.04.2019 Deadline for master's thesis submission: 19.08.2019

Assignment valid until: _____

Ing. Michal Jasný
Supervisor's signaturedoc. Ing. Oldřich Vitek, Ph.D.
Head of department's signatureprof. Ing. Michael Valášek, DrSc.
Dean's signature

III. Assignment receipt

The student acknowledges that the master's thesis is an individual work. The student must produce his thesis without the assistance of others with the exception of provided consultations. Within the master's thesis, the author must state the names of consultants and include a list of references.

3.5.2019

Date of assignment receipt

J. Vijay

Student's signature



Declaration statement

I declare that this diploma thesis work has been written independently by myself under the guidance of Ing Michal Jasný using the works of literature and resources and all the external resources are acknowledged in the list of used references.

In Prague

19.08.2019

Vijay Jeyaraman



Acknowledgement

I would like to thank my supervisor Ing Michal Jasný for continuous support, feedback, motivation and for providing the experimental data from the test bench. Furthermore, I would also like to thank doc. Dr. Ing. Gabriela Achtenová for teaching and providing enough knowledge to understand the transmission functions in real-time. I would like to thank doc. Ing. Michal Hajžman, Ph.D. Faculty of Mechanics Engineering, the University of West Bohemia in Pilsen for the simulation support. His guidance helps me to understand the ADAMS software background theory and how to approach simulation to get solutions. Finally, I would like to thank my classmates and friends, who supported me technically and emotionally for my thesis work.



Annotation

Author name	Vijay Jeyarman
Thesis name	Gearshift simulation model of a dog clutch
Academic year	2018/2019
Study program	Master of Automotive Engineering
Institute	Department of Automotive, Combustion Engine, and Railway Engineering
Thesis supervisor	Ing. Michal Jasný
Simulation Consultant	doc. Ing. Michal Hajžman, Ph.D.

Bibliographic information:

Number of pages	80
Number of pictures	46
Number of tables	10



Abstract

This thesis is mainly focused on the dog clutch engagement process with a trapezoidal dog which can eliminate the bounce-back effect and reduce radial backlash between dog clutches. The main objective of the thesis was to model a dog clutch using appropriate multibody simulation software to understand the engagement process with different relative angular velocity and shifting force. The simulation model must show a dynamical response and behave very close to reality.

In the first part of the study, a brief explanation of the dog clutch principle, engagement condition, application area, bounce-back effect, gear shifting process and previous research work on dog clutch are discussed. After that multibody simulation software basics, and background theory are explained.

In the second part of the study, given experimental data were analyzed to get useful information that information integrated with simulation. The experimental results are mainly focused on the engagement time depending on the relative angular speed difference and gear shifting force. After that dog clutch model was created in the chosen multibody system dynamics software and the corresponding results are taken out. Finally, the simulated results are validated by comparing with measured experiment data.

Keywords: Moment of inertia, Multi-body simulation, Dog clutch, Bounce-back, Material stiffness, and damping coefficient, Static and dynamic friction coefficient, Stiction and friction transition velocity, Relative angular velocity, Gear shifting force, Joint and Constrains



Contents

1. Introduction	1
1.1 Motivation.....	1
1.2 Modelling and Simulation	3
1.3 Objective of the thesis.....	4
2. Technical Background and Related work	5
2.1 Dog clutch	5
2.2 Prior work on dog clutch at CVUT.....	14
2.3 Experimental setup for measurement	19
2.4 Multibody Simulation	22
3. Experiment testing and analysis	33
3.1 Testing.....	33
3.2 Analysis.....	34
4. Dog clutch modeling and simulation	38
4.1 Creating MBD model	38
4.2 Sensitivity analysis of the parameters influence.....	45
4.3 Solver for nonlinear contact dynamic simulation	48
4.4 Simulation results	50
5. Dog clutch model validation	52
5.1 Reason for lower average engagement time in simulation	52
5.2 Future work.....	55
6. Conclusion.....	56
Nomenclature and abbreviations	57
References	60
List of Figures	62
List of Tables	65
List of attachments	66
Appendix	67
Validation results	67
Design of Experiment results	71



1. Introduction

1.1 Motivation

Over the decades, the automotive driveline developments have changed drastically to satisfy the customer requirement and hold the position in the market. More and more development makes the transmission as a complicated system and increases the transmission mass. From the point of the gearbox cost, it increases with weight.

If we look back to the history, old gearboxes were engaging the gear by sliding the gears on each other which requires only fewer components but need careful engagement timing. The main drawback of this transmission is, the gears start to bounce off each other when the relative angular speed difference is high. During the gear changing loud noise is generated by gears and there is a high chance of wear and tear of the gearbox. To avoid these drawbacks, the modern manual transmission is always equipped with speed equalizing mechanisms such as synchronizer, multi-plate clutch, and break.

The synchronizer can provide smoother gear engagement and gearshift comfort. However, synchronizer has some downsides:

(I) In order to get this advantage, synchronizer should equip with cone, blocker ring, sleeve and hub which takes more longitudinal space in gearbox.

(II) the friction material, such as brass, in synchronizers is more prone to wear and breakage than gears, which are forged steel, and the simplicity of the mechanism improves reliability and reduces cost.

(III) the shift time is limited by synchronizer capacity. The increase of capacity of synchronizer leads to an increase of complexity or to solutions which are advantageous only in some special gearbox designs. [1]

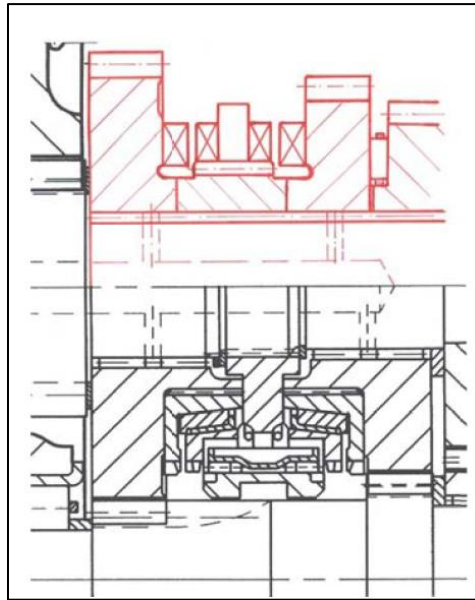


Figure 1 - Comparison of dog clutch and synchronizer [1, p. 3]

The current automotive industry forced to make the vehicle to reduce weight by downsizing and downspeeding to increase fuel efficiency and reduce emission. If the weight of a vehicle is reduced by 10%, fuel efficiency is improved by about 3 to 8%, acceleration performance is improved by 8%, and the emission of environmental pollutants is also reduced [2]. By replacing the synchromesh unit with a dog clutch system in manual transmission, which does not affect the transmission efficiency and reduce weight and space in the longitudinal direction. It is especially helpful for hybrid vehicles. Unlike the synchromesh, the dog clutch engaged without synchronizing mechanism, which reduces the transmission length. A dog clutch, if successfully implemented in manual transmission with better engagement, then it provides better packaging and reduces the transmission overall weight.

The dog clutch system is a significant success in racing and two-wheel motor vehicle but it's very rare in the passenger car vehicle. To successfully implement the dog clutch in a passenger car, the dog clutch design must take several requirements into account: Gear shift comfort, engagement time and rattle noise. Gear shift comfort is important to design criterion for all passenger car transmissions. From the point of shift comfort, the gear shifting process should be easier and should not take much time to engage the gears. Otherwise, there is a risk of losing the engine speed that will lead to more emissions from the vehicle.



Every positive design contains the seeds of equal negative events. The dog clutch engagement also contains some negative events:

- i. the dog clutch engaged without synchronization mechanism which leads to producing noise.

This can be avoided by using an external synchronization device which can reduce the relative speed difference between dog clutches during the engagement period.

- ii. the bounce-back effect considered a problem that appears during the engagement process and It negatively influences the engagement time and driving feel.

Therefore, a proper and good dog clutch performance is very important to achieve the desired gear shifting. In this thesis work, the dog clutch is designed with a trapezoidal dog to reduce the above-mentioned flaws.

1.2 Modelling and Simulation

The experiment typically requires multiple dog clutches with gear wheels and expensive instrumentation to obtain indicative data on all the relevant parameters, and after all this, there is still a possibility that the results show that the desired results cannot be obtained thus making the whole experiment a waste of resources, but virtual simulation doesn't.

The modeling and simulation tools have the power to reduce the cost and time of the experiment. There are several methods to simulate the behavior of a gear shifting such as mathematic modeling (MATLAB), Finite element method (Ansys) and multi-body dynamics (MSC ADAMS, SIMPACK). The last approach seems to be the most suitable for a dog clutch engagement process because it allows to the analysis of the contact force in the time domain.

The multibody simulation is the best approach to study the dynamic behavior of the dog clutch before conducting the experimental test. So, MBD is the first step to analyze and optimize the gear shifting process. It is useful for sensitivity analysis of each parameter that after the gear shifting process. Furthermore, the MBD can provide visualization and information at each point to point engagement as well as gives a clear insight into the system.



1.3 Objective of the thesis

The main goal of the thesis work is to develop the dog clutch gear shifting model in an appropriate multibody software then compare these simulated models with the experiment model. To achieve these goals, the following objectives are defined:

- General study of Dog clutch and corresponding gear shifting method
- Choose an appropriate simulation software for a gearshift simulation model of dog clutch engagement e.g. Simpack, MSC ADAMS
- To study the background theory of chosen multibody simulation software using the reference material
- Build the geometrical model in a CAD software
- To build a concept of a virtual multibody model of dog clutch gear shifting in a chosen MBD software
- To validate the simulation with the experiment result.

2. Technical Background and Related work

2.1 Dog clutch

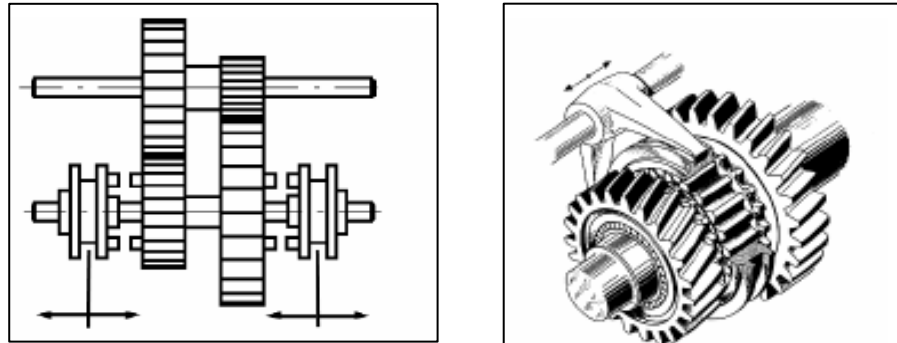


Figure 2 - 2 speed gearboxes with dog clutch [3, pp. 15, 301]

In transmission, there are two types of clutches used. A distinction is made between friction clutches and positive locking clutches e.g. dog clutch.

Firstly, friction clutch which allows for a slip between the driving side and driven side and such a connection can be provided non-positively by means of friction. These components are expensive to manufacture and takes much construction space in the gearbox. These friction clutches are commonly used in automatic transmission. However, the drag loss and slip between the clutch reduce the efficiency of the transmission.

Secondly, dog clutches are used to connect two rotating or drive components by the principle of the interface between the component in the coaxial direction around an axis of rotation. The dog clutch is used to either connect or disconnect components and both driving and driven side to rotate at the same speed and never slip. The dog clutch is an alternative to the synchronizer and it only requires a small amount of axial construction space.

2.1.1 Dog clutch applicable place

The transmission with a standard dog clutch cannot be used for all the places because it always comes without synchronizing mechanism. The standard dog clutch is more compact and saves space and weight. However, there is some application area still dog clutch is used:

- In the clutch-controlled power take-off unit, the auxiliary unit is connected by a dog clutch

- In most of the trucks have rear-wheel drive and front wheels are free to rotate. This two-wheel drive arrangement can be changed into four-wheel drive using the dog clutch which is positioned inside the transfer case. The engagement and disengagement of the dog clutch can be controlled either by the driver using a shift lever mechanism (or) the transmission control unit.
- The open differential split drive torque symmetrically to both wheels. When the frictional potential of the two drive wheels is different, the propulsive forces transmitted to the road surface for both drive wheels depend on the smaller frictional potential of the two. At this condition, the vehicle cannot move off. In order to overcome this disadvantage, the differential gears equipped with a dog clutch to lock the differential and this makes the axle rigid again. The rigid axle transfers a different amount of torque to both wheels. [3]

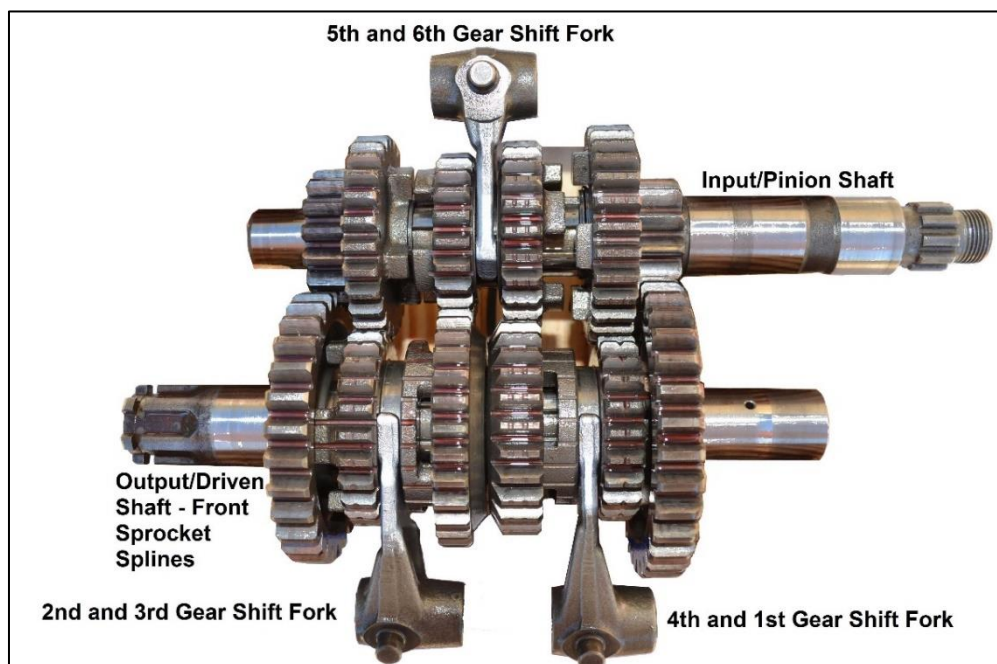


Figure 3 - Motorcycle gearbox [4]

- The dog clutch gear engagement mainly used where synchronizers cannot be possible especially at commercial vehicle gearbox. In heavy-duty vehicles, the main gearbox is unsynchronized and is shifted with dog clutches. If the main gearbox unit provided with synchronizer then the service life of the gearbox starts to reduce. But the splitter and range change unit are synchronized.

- The axial construction space for the dog clutch is less compared to the synchronizer. So, the dog clutch utilized where not enough space for transmission. Example: Motorcycle. The motorcycle gearbox is called sequential manual gearbox because gears are selected in order and direct access to the specific gear is not possible (1-N-2-3-4-5). [5]
- Even we can see dog clutches in the racing gearbox with radial backlash. The dog clutch in the racing gearbox reduces the gear engagement time and decreases the transmission weight.

2.2.2 Engagement condition

I. The minimum distance at which both half clutches can engage [6]

$$Z = h + Z_{gap}$$

Where

Z – overall clutch displacement

h – dog height

Z_{gap} – Clearance between two half clutches

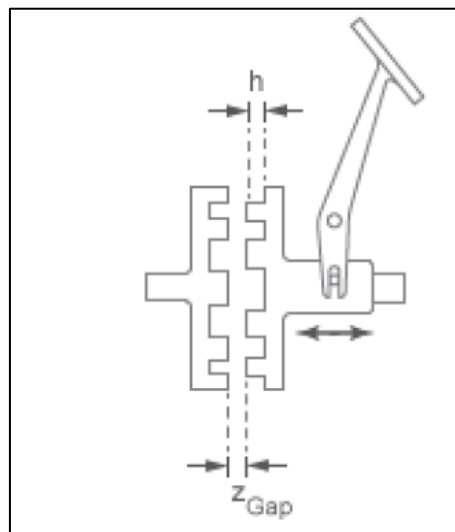


Figure 4 - Dog clutch overall displacement [6]

II. The engagement of the dog clutch can take place, only if there is a relative speed difference between dog clutches and this speed difference describes how fast dog clutches are slipping each other

$$\omega_{rel} = \omega_1 - \omega_2$$

2.1.3 Engagement Cases

Case-1 Both rotate at synchronously $N_1 = N_2$

In this case, both clutches halves rotate at the same speed, the crest or tip of the half clutch contact with a trough of another half clutch. For rectangular dogs without face chamfer, clutch halves working sides may come in contact however, clutch halves will not become engaged because relative angular speed different between clutches are zero and its illustrated in figure 5. In the example, the sliding dog displacement at final engagement is 4.7 mm but after the first face to face contact at 1.6 mm, two dog clutches are not slipping each other. Without relative angular speed difference, the clutch adjustment will not happen, and the working side of the dogs not engaged over their entire height. At this condition, it should not fulfil the engagement condition I and II.

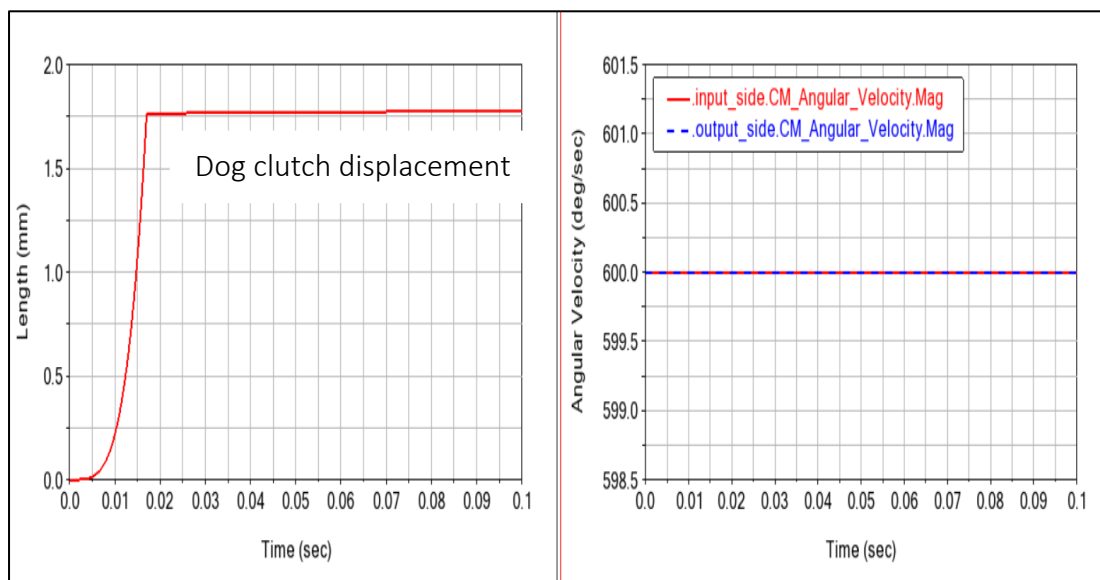


Figure 5 - Permanent face to face contact

Case-2 Driven half clutch lags $N_1 > N_2$

The driving half clutch rotates faster than driven half clutch because of this relative angular speed difference dog can insert their entire height. If $N_2 = 0$ then the tire starts to slip and stop the vehicle. Furthermore, at this condition, the probability of dog engaged over their entire height is high and this is the most favorable condition for clutch engagement.

Case- 3 Driven half clutch overrun $N_1 < N_2$

In this case, driving half clutch rotates slower than the driven half clutch. After-engagement, slow down occurs because half clutch direction of rotation opposite to another half clutch. [7]

2.1.4 Quality factor

1: Gear shifting time and comfort

From the point of shift comfort, gear shifting time must be reduced as much as possible. But the following effect can be considered a problem that appears during the engagement process that negatively influences engagement time and driving feel.

2: Bounce-back effect

When two half clutch dogs start to contact at face to face, sliding half clutches start to bounce-back due to the material stiffness, damping and relative angular velocity.

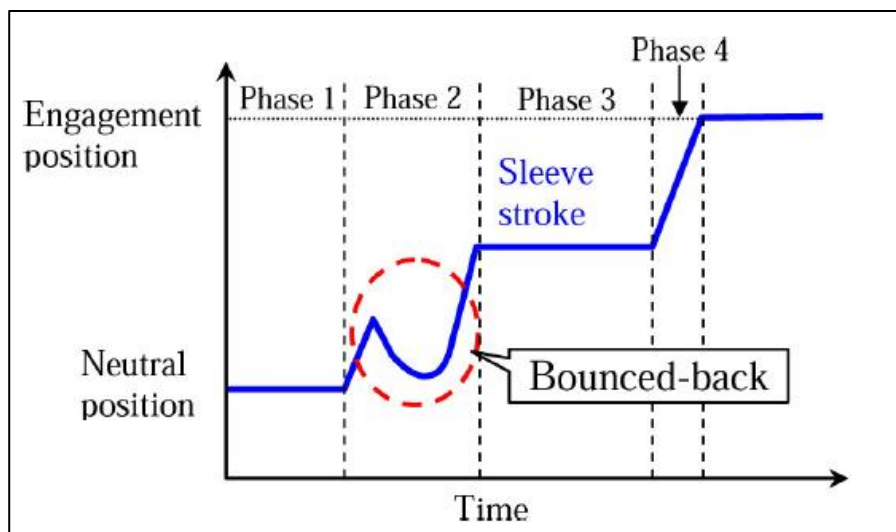


Figure 6 - Bounce-back effect [8, p. 4]

If the bounce-back occurs the gearshift time becomes to be longer because the dog skips the correspond slot and jump into the next slot. This kind of bounce generates metallic noise and produces axial vibration on the clutch. A bounce-back occurs, when two half clutches rotate at high angular speed difference and it mainly depends on a number of dogs, the thickness of dogs, relative angular velocity and face of the dog.

2.1.5 Gear shifting process for rectangular dogs

The dog clutch engagement process can be divided into four phases. The dog clutch would not engage without relative angular velocity (or) mismatch speed already discussed in chapter 2.1.3 except when dogs are positioned against slot. The stages of the shifting process of the dog clutch are shown in figure 7.

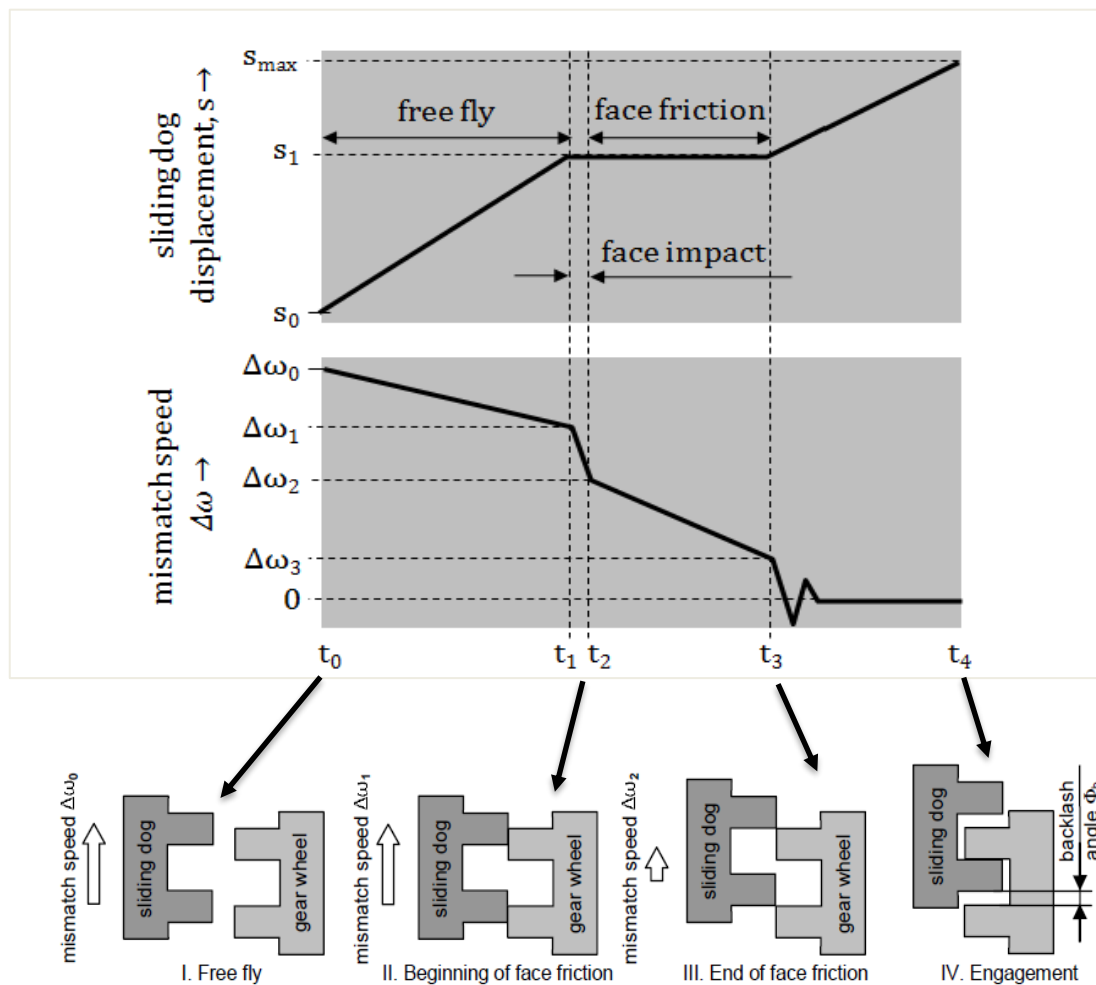


Figure 7 - Engagement process of dog clutch [9, p. 2]

Phase-1 Free fly

The gearshift force is applied to the shift sleeve and the sliding dog starts to move towards the gearwheel at the time t_0 with initial relative angular velocity considered as $\Delta\omega_0$. Due to the friction loss and slight change in vehicle speed, the relative angular velocity changes from $\Delta\omega_0$ to $\Delta\omega_1$.

Phase-2 Face to face contact

In this phase dog to dog contact occurs with high impact. The high impact force stops the sliding dogs by consuming the motion energy and the energy consumption depends on the material damping coefficient. As a consequence, the face contact between dog clutches generates frictional moment which acts against the relative angular velocity. The peak frictional moment causes the relative angular velocity drops sharply to $\Delta\omega_2$ at very short period of time.

Phase-3 Face Friction

After the impact, the face areas slip on each other, until the dog turns against the slot by the time t_3 . Again, due to the face friction torque, relative angular velocity reduced to $\Delta\omega_3$.

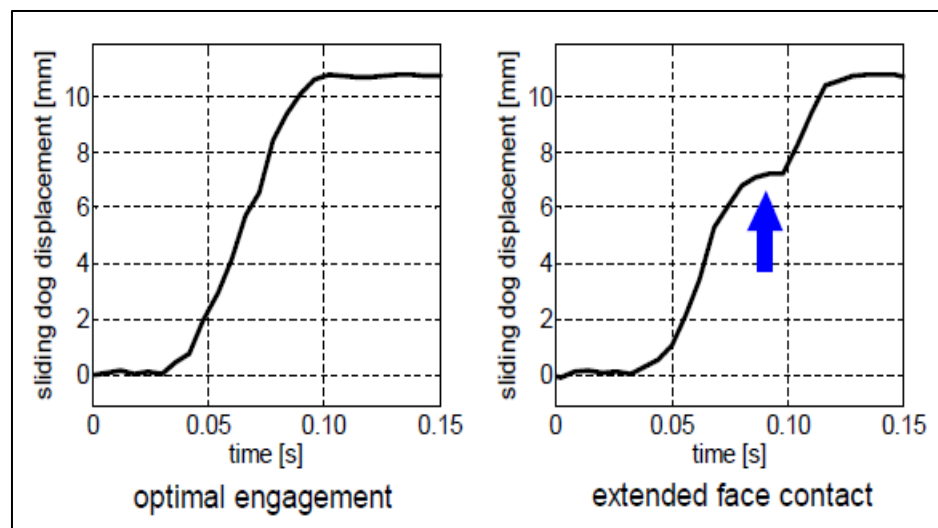


Figure 8 - Dog clutch initial contact position

(a) face to slot contact

(b) face to face contact [9, p. 2]



Phase-4 Engagement

The dogs in the clutch free to enter the corresponding slot of the counterpart, the dog clutch engages, and relative angular velocity reduces to zero. The different angular velocity will cause the torsional vibration and the amplitude of vibration depends on the backlash angle and relative angular velocity [9].

If the sliding dogs are placed exactly against slots, then engagement happened without Phase-2 and Phase-3 and there would be no face to face to contact. Suppose it is the case then engagement time reduce as shown in Figure 8 - (a)

2.1.6 Dog clutch Design possibility

The dogs are in contact with each other to transfer the force in the circumferential direction when the clutch is engaged. So that the corresponding dog clutch with mating surfaces contact is formed only in the direction of the force.

The dogs can be modeled symmetrically or asymmetrically with regards to mating surfaces. The symmetry of the dogs depends on the design of the dog insertion slope. The symmetry profile gives better torque transmitting in either direction of clutch rotation: Traction (or) driving and braking. The driving and braking side of the contact surface area in the dogs are the same.

For making trapezoidal dogs, two insertion slopes can be formed on a dog, each directed at a contact surface. The trapezoidal dog can possible to provide a sufficiently large contact surface and this contact surface area can change according to the insertion slope angle of the dog.

There are three types of dog clutch design that can be defined by the angle of the contact sides.

(I) Zero slop angle

The zero-slop angle corresponds to the rectangular shape dog clutch. The rectangular dog is used less frequently because of difficulties in engaging such clutches, both when stopping and while driving and because it is impossible to obtain a clearance-less coupling of dog.

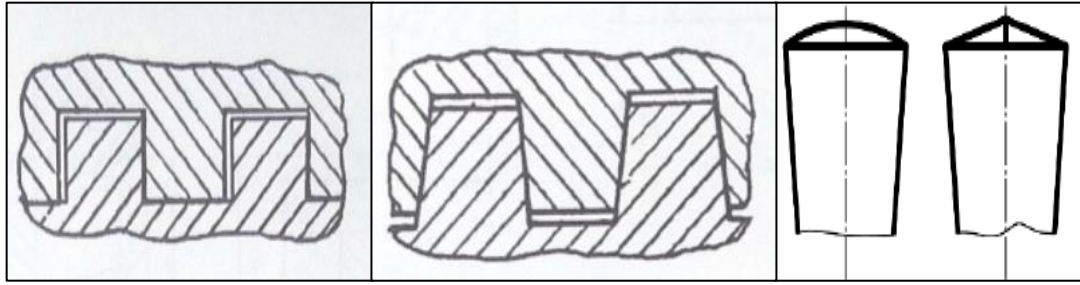


Figure 9 - Dog design according to the insertion slope

Zero slope [7, p. 243]

Positive slope [7, p. 243]

Negative slope [3, p. 303]

(II) Positive slope

The positive slope dog clutch is used in the transfer case and differential locking for heavy-duty vehicles. The lateral clearance is eliminated when the dogs move in an axial direction which gives better engagement. However, the axial force is generated during the torque transmission leads to continuous self-disengagement. If the inclination angle is very low, the dog clutch self-locks each other.

(III) Negative slope

The negative slope dog is used in synchromesh gearbox. When the gearshift force applied to the shift sleeve, the dog in the sleeve engage with dogs in the synchronizer ring and prevent the disengagement during the torque transmission. After the gearshift sleeve positively engages, the friction torque acts to lock the synchronizer and is opposed by an opening (or) index torque resulting from the decomposition of forces in dog surface. As long as there is a speed difference, the locking friction torque is greater than the opening torque. If the dog bevel angle falls below the safe lower limit, then grating occurs. If the opening angle exceeds the upper limit, the gear shifting effect increase and shifting comfort suffers. [7] [3]

2.2 Prior work on dog clutch at CVUT

This chapter review previous research work on dog clutch at CVUT. The main purpose of the review is to understand how the dog clutch mechanism evolved in each research work.

2.2.1 Smoothness of Maybach dog clutch

In this research work mainly focus on design and test the Maybach dog clutch in passenger car gearbox with external synchronization. The designed Maybach clutch replace the place of existing synchronizer in the passenger car gearbox between 3rd and 4th gear. The external synchronization device used to set up the relative speed between the free rotating wheel and shaft. The prototype of the Maybach dog clutch illustrated in figure 10.

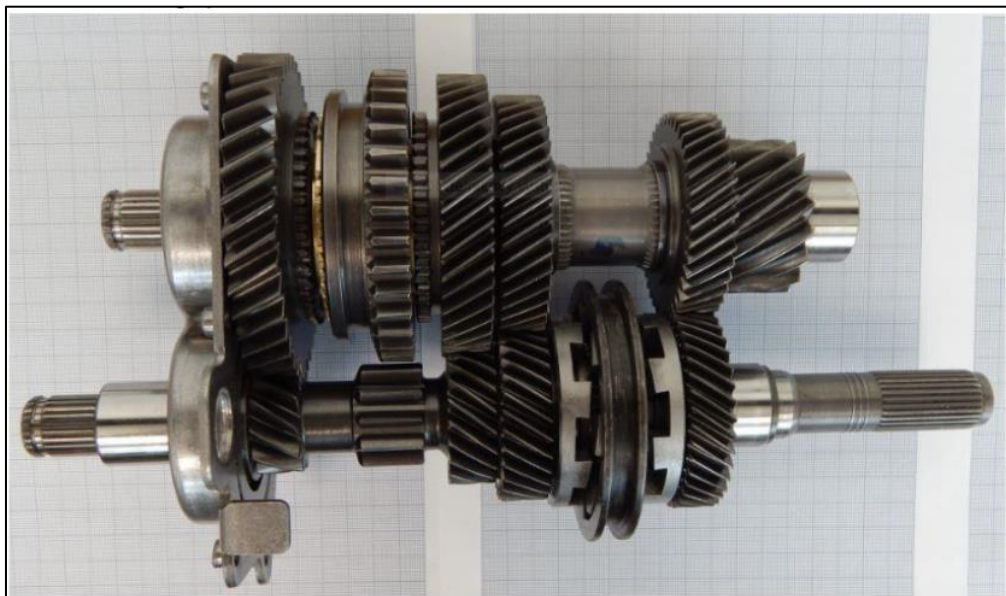


Figure 10 - Input and output shaft of the passenger car gearbox with Maybach dog clutch between the 3rd and 4th speed [1, p. 4]

The corresponding dog clutch results were compared with classical shift synchronizer. To compare the results tried to keep the gearbox with as fewer changes as possible: the same gearwheels with the same diameter where the dogs are positioned, the same distance between the pair of gearwheels engaged by one shift clutch and same shifting force, etc.

The gearshift test was conducted on the inertia test bench. In the test bench, the dog clutch was shifted 1500 times from natural position to engaged 3rd gear. The shift smoothness was elevated by the vibration measurement. The acceleration was

measured on the gearbox casing above the bearing on the input shaft, in both radial and axial direction. The Maybach clutch was disassembled and observed after 500 engagement to find wear rate in dog faces and the results were slight chamfering on the sliding sleeve. The RMS and maximal acceleration values from Maybach clutch and classical synchronizer were almost same and comparable till 500 rpm. The Maybach clutch ensures, that the gears can be shifted at any time. The results from the Maybach clutch was good and it leads to the continues research in dog clutch. [1]

2.2.2 Pakoshift

The pakoshift dog clutch was a bit complex because of two different dog designs used for engagement.

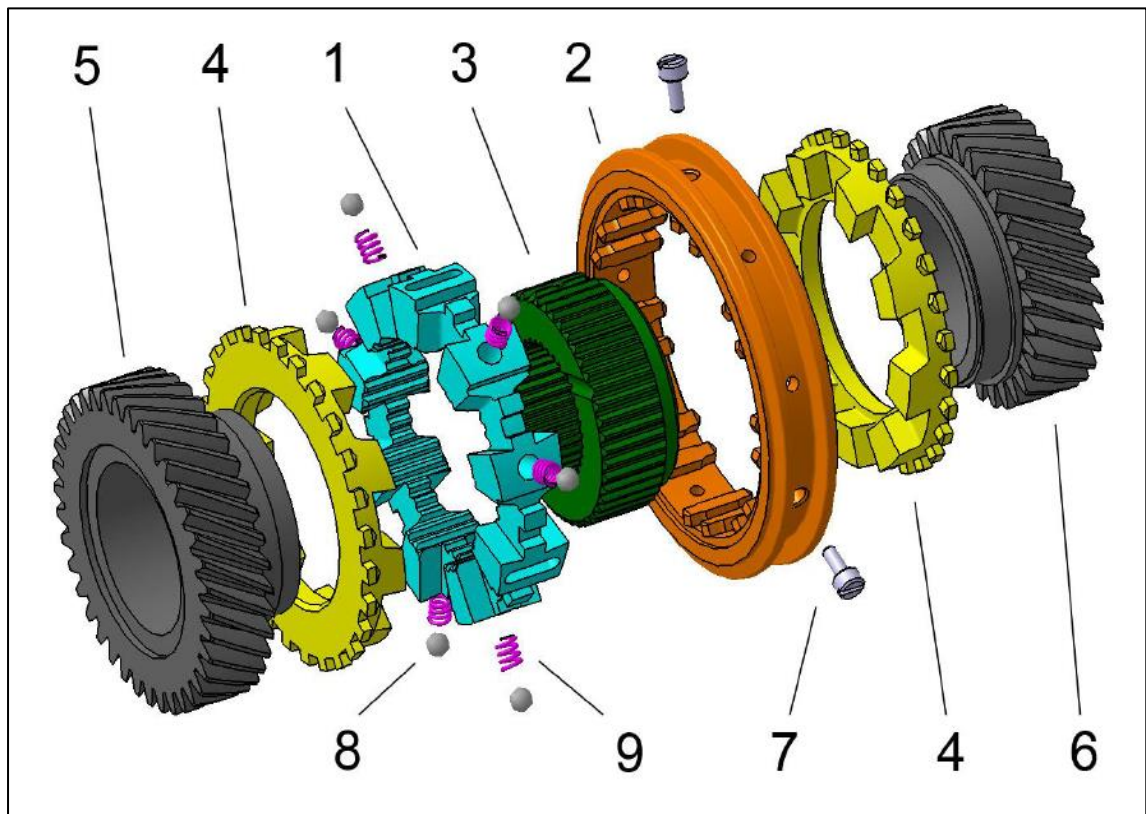


Figure 11- Exploded view of Pakoshift clutch

1- Ring with shifting dogs, 2- Gear shift sleeve, 3- Clutch hub, 4-Counter dogs, 5+6- Free rotating wheel, 7- stop pin, 8- Detent ball, 9-spring [10, p. 35]

First dog clutch designed with a negative flank angle and used to transmit the transmission torque to the wheel. Second dog clutch comes with a positive angle, used to lock the shift sleeve to prevent the disengagement.

The assembly exploded view shown in figure 11. The sliding dog placed on the clutch hub which can slide in the axial direction and the hub forms a link between the shifter and the shaft. Instead of classical synchronizer ring, claw rings (or) counter dogs were placed on the gearwheel, the dogs of the front dog clutch, circumferentially securing the dogs defining the clearance. When shifting process starts, the shift sleeve moves towards the gear wheel. The shifting of the front dog clutch engages with the counter dog and transmit the torque to the wheel. After the front dog full engagement, the shifter can no longer move but the clutch shifting process itself is not yet finished. At this stage relative angular velocity is almost reduce to zero.

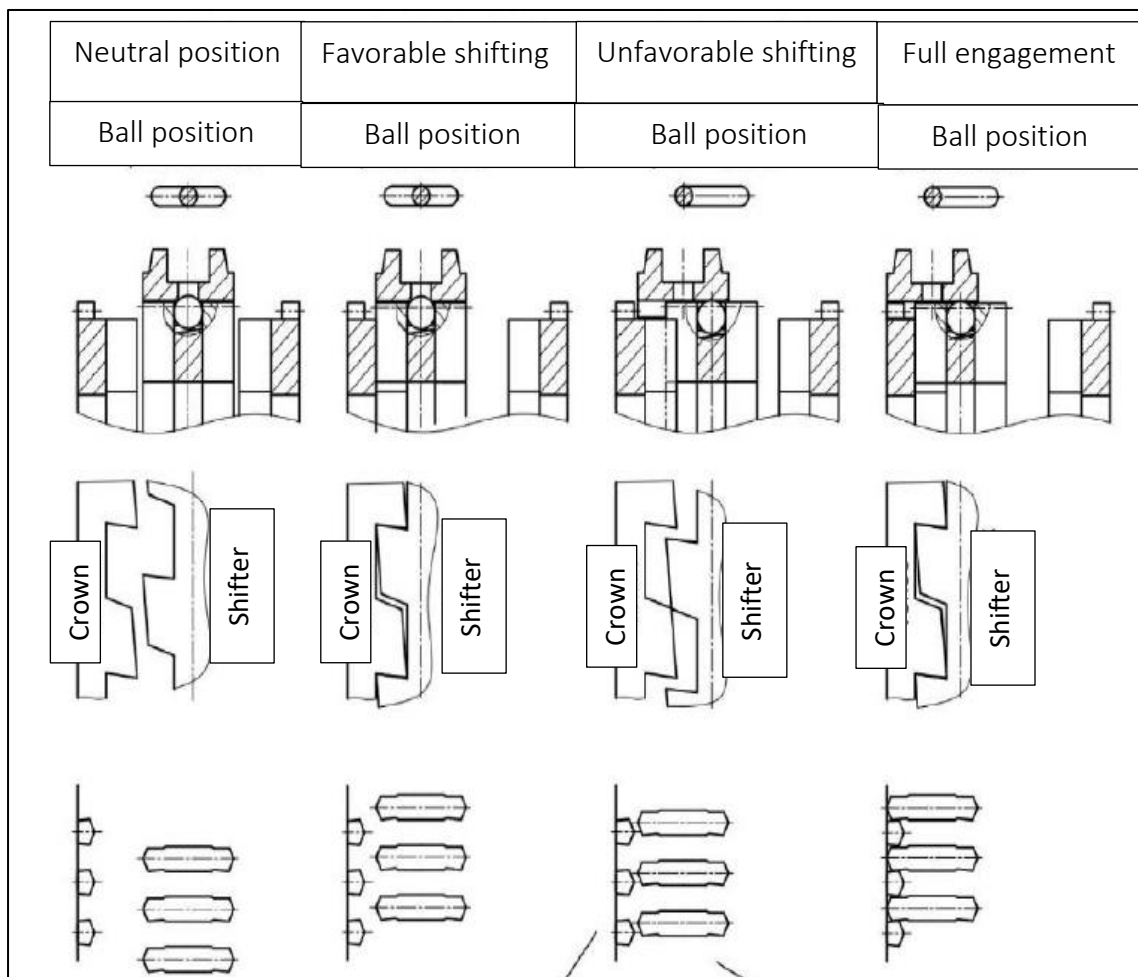


Figure 12 - Shift Sequence of Pakoshift [10, p. 36]

The locking mechanism in the Shifting dog resists the further movement of the shift sleeve. The shifting force should overcome the locking mechanism, for further movement of the sleeve. When shifting force overcome the spring resistance, it starts to push the ball into the shifter and the sleeve spline engages in the locking dog, along the claw ring circumference. [10]

2.2.3 Dog clutch with blocking mechanism

In this research, the dog clutch was designed with tapered contact faces. The geometry of the dog gives a better engagement process and minimize the radial backlash after the engagement. However, during the engagement process dog produce an axial force on the contact face due to the shape of the dog. This axial force could not allow the dogs in the engagement state. It tries to push the sliding dog and leads to disengagement of the clutch. Therefore, a separate blocking mechanism was introduced to lock the dog clutch to prevent disengagement.

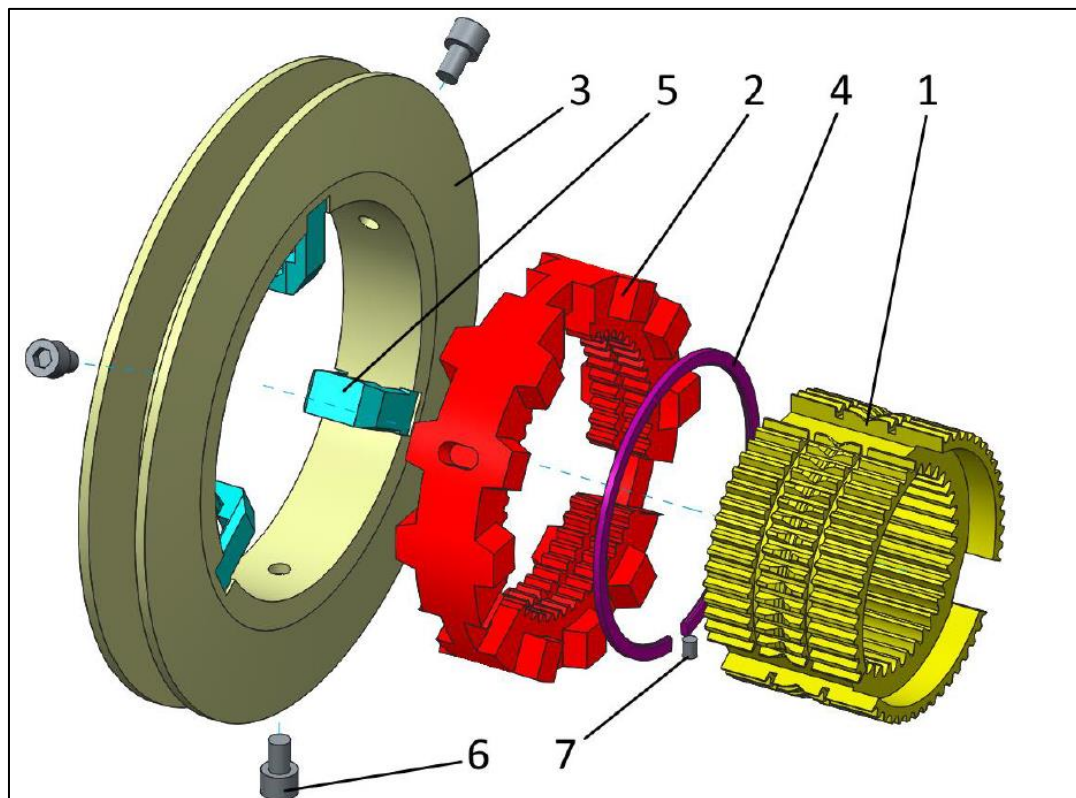


Figure 13 - Exploded view of Dog clutch with blocking mechanism

1-Clutch body, 2- Sliding dog, 3-Gearshift sleeve, 4-Blocking ring, 5-Gearshift stone, 6- Gearshift pins, 7-Detent pins [11, p. 3]

The dog clutch consists of the clutch body which is fixed with a gearbox shaft using the internal spline. The sliding dog placed on the clutch body which can move axially. The counter dogs are fixed with gearwheel. The movement of the dogs controlled by gearshift sleeve through gearshift pin. Gearshift stones are fixed to the gearshift sleeve. Blocking rings are placed in the clutch body grooves and cannot rotate freely around the clutch axis of revolution due to detent pins. However, the internal diameter of the blocking rings is bigger than the external diameter of the grooves. As a result, the C-shaped blocking rings can shrink slightly when under pressure of the gearshift stones.

The beginning of the gear shifting sliding dog is placed in the neutral position and blocking rings are in non-compressed state. The sliding dog cannot move until the blocking rings are compressed and this is achieved by providing gearshift force on the shift sleeve. The applied gearshift force compresses the blocking ring through the gearshift stone by the axial moment of the gearshift sleeve.

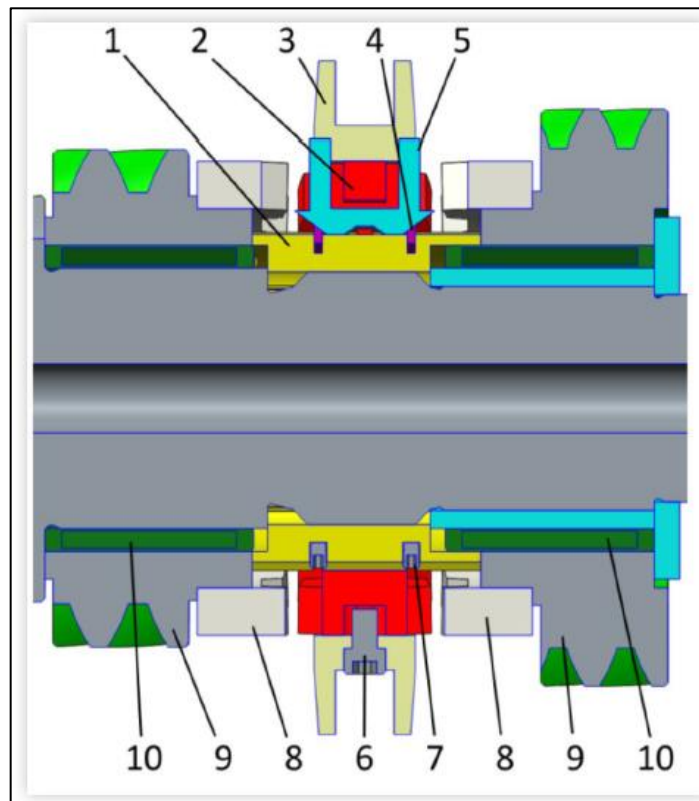


Figure 14 - Dog clutch at neutral position [11, p. 4]

8- Crowns with face dog, 9-Ideler gear wheels, 10-Needle bearing



Once the rings are compressed, then the sliding dog easily moves with sleeve and engage. After the engagement, the gearshift stone no longer holds the blocking ring in a compressed state due to the stone geometry. The blocking rings back to the original shape and fits into the grooves in the sliding dog. Thus, sliding dog cannot disengage once it is engaged without any external force on the sleeve. [11]

The dog clutch with trapezoidal dog minimizes the radial backlash which can avoid the dog to dog clash during the engagement. The blocking mechanism prevents the clutch disengagement after the engagement and holds the sliding dog in a neutral position. My diploma thesis work is the continuation of this research work. Further work on this research gives more quantitatively result.

2.3 Experimental setup for measurement

The inertia test bench measurements are aimed at exploring gear shifting and performance of selected gearbox under predefined boundary condition which allows to find gear engagement time and effectiveness of the gearbox. For the test stand design, the main requirement was to keep the design as simple as possible by keeping a similar functional condition as in a real vehicle. [12]

The inertia test bench at CTU laboratory consists of a MQ 200 FCU single-stage gearbox combined with the flywheel on its axis of rotation which represent the vehicle inertia. The moment inertia of flywheel of the test stand is 15 Kg.m^2 . This value was chosen as an optimum between the demand of inertia representing the passenger car, and the demand for low inertia, which can be fast accelerated or decelerated to minimize the technological time for endurance tests.

The inertia flywheel is driven by AC electrical motor controlled by frequency converter with the range 50 Hz for current test bench, but also can work at 60 Hz, according to which the speed is required. The input shaft of the gearbox is not connected with the engine because, in the period of gear shifting, engine disconnected by the friction clutch as well as engine torque does not affect the gearshift process but to control the input shaft speed, another end of the shaft connected with a small electric motor.

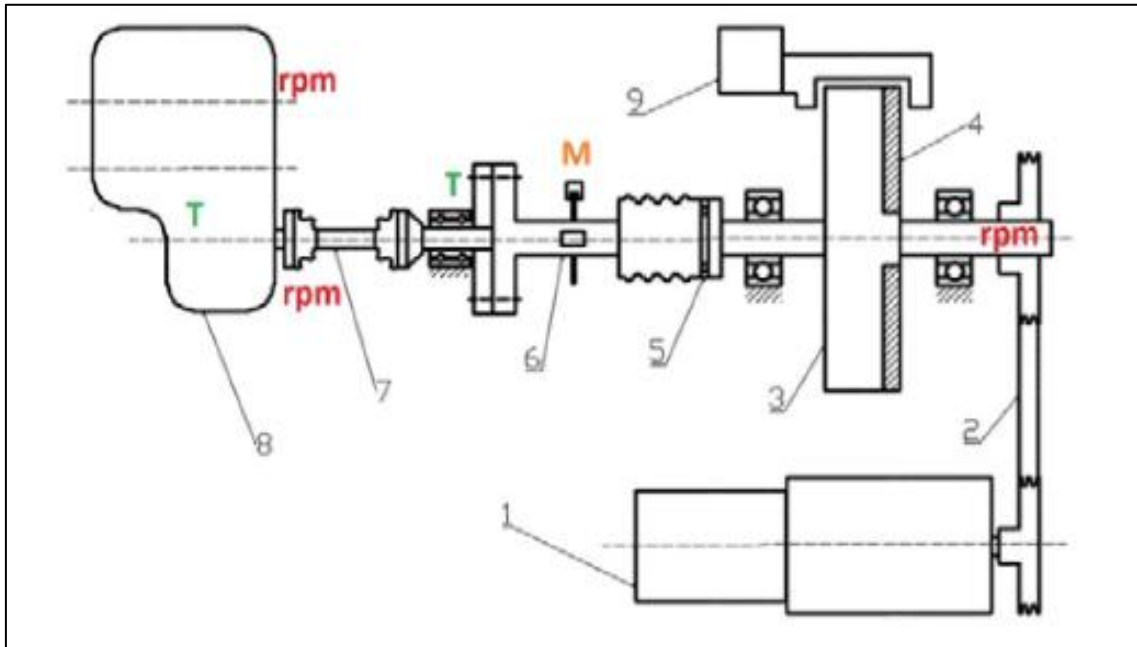


Figure 15 - Scheme of the inertia test stand.

Legend: 1- Electric motor, 2-Belt drive, 3-Flywheel, 4-increase of inertia via external disc, 5-Safety and flexible coupling, 6-Strain gauge with telemetric device+ RPM measurement, 7-Driveshaft, 8- Tested gearbox, 9- Safety brake, rpm- Sensor for speed of rotation, M- Torque sensor, T- Temperature sensing [12, p. 3]

The pneumatic robot arm placed outside the gearbox to actuate the gear shifting process. Both simulation model and experiment are conducted and validated during upshift from natural to 3rd gear.

There are many variants of the MQ200 gearbox whose number of dog configurations are different. Currently, the FCU type is used, whose specification is given in the table below

Gear speed	1	2	3	4	5	R1	R2	Differential
Number of dogs on input gear	11	21	31	39	48	24	11	17
Number of dogs on output gear	44	43	40	39	38	35	24	66
Gear ratio	4.00	2.0476	1.2903	1.00	0.7917	1.4583	2.1818	3.88

Table 1 - Gear ratio of tested gearbox

Two types of experiments have been performed to analysis the dog clutch engagement. The first experiment is considered as the vehicle in traction mode, in this experiment driving side of the dog surface contact with the driven side of the dog surface. In the second experiment vehicle in braking mode, in this experiment braking side of the dog surface start to contact.

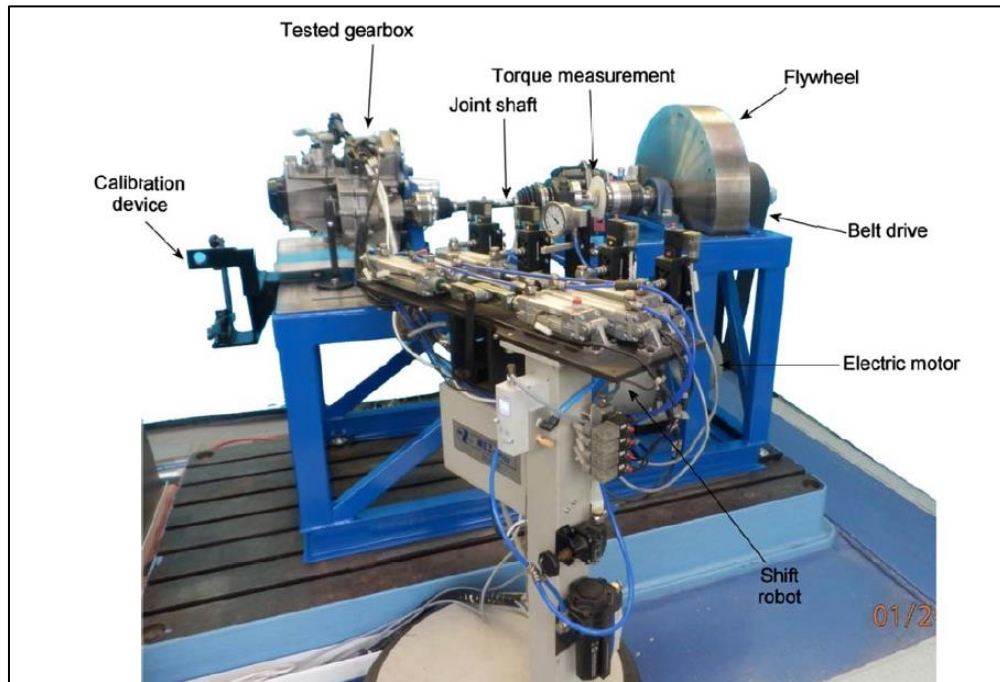


Figure 16 - Flywheel inertia test bench

The measurement sensors are not perfect and will be affected by electrical noise, environmental condition and procedures. In the test bench has uncertainty associated with it and some of the uncertainties are unavoidable. To compare the measured data with simulation result, they must trace back to a common reference.

Sources of uncertainty in the experiment:

(I) Sleeve displacement not measured inside the gearbox instead of measured at the robot arm. When the sleeve displacement measured at the robot arm, the measurement does not show an intermediate phase of the dog clutch engagement process

(II) the gear shifting force also measured at the robot arm

(III) during the dog clutch engagement, an angular position of the dog clutch cannot be control, meaning we cannot define whether its face to face (or) face to slot contact. These measurement inaccuracies make very difficult for DOE. The process of DOE explained below in chapter 4.2.2.



2.4 Multibody Simulation

There are several commercial MBD (Multibody system) software that were developed last four decades such as MSC ADAMS, SIMPACK, LMS DADS etc. The choosing the best MBD software for gear shifting is very important otherwise the simulation could not be comparable with the experiment result. For that reason, one of my thesis tasks is to choose an appropriate MBD software to analysis the dog clutch engagement process and the selected software should simulate the gear shifting as real as possible.

At the beginning of thesis work, I prepare to use Simpack because Czech Technical University in Prague has a license for Simpack. The Simpack is composed with high accuracy integrator which gives good results but Simpack is little bit resisted software and could not find any reference (or) resources in the internet. Without reference making computationally more efficient model is very difficult especially defining the solver parameters such as error, integrator and integrator time step.

As per the modeling, the dog clutch model has to be set up as nonlinear spring-damper model but the geometrical contact in Simpack acts like a linear spring-damper model and it does not give the realistic simulation results. The difference between linear and nonlinear spring-damper model is explained below in equation number (13). It would be complicated to convert linear to nonlinear spring-damper model and Coulomb friction to regularized Coulomb model.

Therefore, I chose an MSC ADAMS as an alternative of Simpack because ADAMS uses the nonlinear contact algorithm between the dog. Furthermore, I got help from the University of West Bohemia in Pilsen, Faculty of Applied Sciences. They gave an idea of how to approach the MBD software as well as provide a reference of ADAMS.

2.4.1 MSC ADAMS

MSC ADAMS (Automatic Dynamic Analysis of Mechanical Systems) is computing software used for modelling, analyzing and optimizing mechanical systems called MBS (MultiBody System). Adams is a family of interactive motion simulation software. ADAMS/Solver can perform six different types of analyses depending on the characteristics of the problem: kinematic analysis, static equilibrium analysis, initial condition analysis, quasi-static analysis, dynamic analysis, linear analysis.



Before using MSC ADAMS, many automotive manufactures conducted a real experiment on the vehicle to study the performance as a function of different parameter settings. The experiments obviously increase time and cost. But using the simulation it possible to compress the cost and time.

2.4.2 Assumptions and Limitations

- In MSC ADAMS, simplification of a dog clutch model is used and other gearbox parts like Shaft, bearing and gearwheels are neglected.
- The dog clutch model is considered as a rigid model and not a flexible model. Consequently, an assumption has been made that the deformation of the bodies can be neglected. Whenever possible, it is preferable to use rigid body models for dynamic simulation because such simulators are invariably more efficient. However, in reality, the dog clutch behaves like a flexible body.
- Lack of knowledge in parameters like material stiffness, damping, static and dynamic friction coefficient ended up with simplification. The design of experiment is conducted to find these parameters optimal value.
- The parameter such as principal mass moment of inertia, rotational speed of dog clutch and gear shifting force values are taken from the test bench.

2.4.3 Theory – Multibody system

2.4.3.1 Global and local coordinate system

A coordinate system is used to measure the quantity result of kinematic and dynamic simulation. Both global and local coordinate systems are providing the relative orientation and position of geometry in space.

Global coordinate system

The global coordinate system acts as an absolute reference frame of the model and this coordinate system is rigidly attached to the ground. If a body is placed in a space, then the corresponding location of the body is defined by three mutually perpendicular unit vectors that specifies three directions. The position and orientation of a body is given by means of global coordinate system.

For example, in figure 17, the vector \vec{R} defines the displacement of point P and R_x , R_y , and R_z are the measure numbers of \vec{R} along the x , y and z axes. The unit vectors \hat{i} , \hat{j} and \hat{k} define the direction. [13]

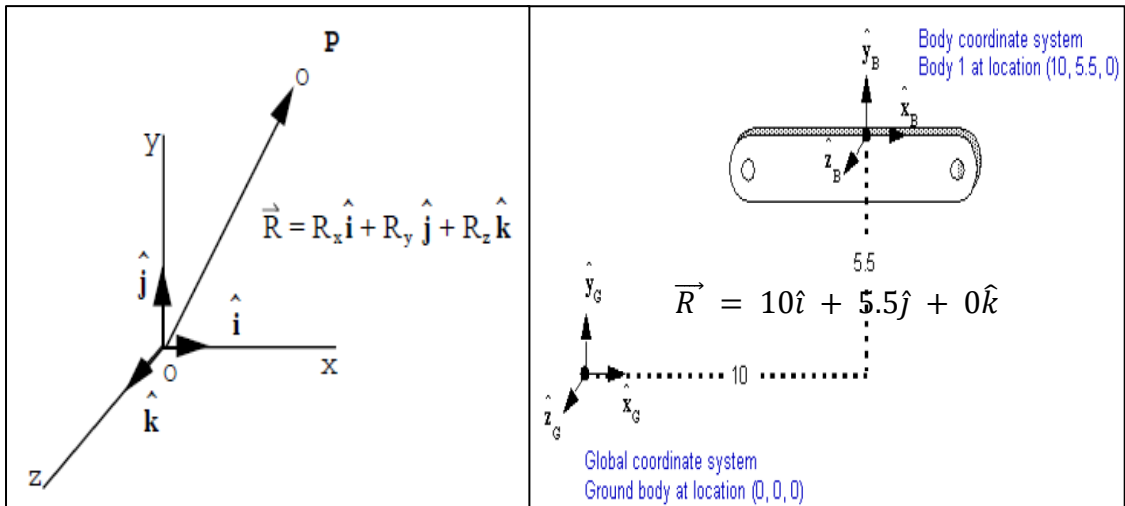


Figure 17 - Global coordinate system and Local coordinate system [13, p. 39]

Local coordinate system

The local body coordinate system is created automatically for each body. When importing a model into ADAMS the initial location and orientation of a body is specified with respect to the global coordinate system. So, each body has a single LBCS and it is not be stationary. The principal mass moment of inertia is defined by using of LBCS.

2.4.3.2 Degree of freedom

Degree of freedom used to describe how the bodies can move in space relative to other bodies. In the mechanical system, if the body place in the space then it has six independent motion: three rotational, three transitional.

On the other hand, constraints and joints are used to remove degrees of freedom and restrict the motion of bodies. Constraints of rigid body systems can be of two kinds: bilateral and unilateral. Bilateral constraints usually take the forms of joints or hinges which serve as the connections between rigid bodies in machines and mechanisms. Unilateral constraints are used to describe collision and/or sustained contact between rigid bodies. Of these two kinds of constraints, the bilateral constraint is easier to model because it can be treated as holonomic constraints and can be directly incorporated into the equations of motion. [14]



To determine total DOF for any system, we can use Gruebler Equation of mobility which is

$$DOF = (6 * \text{Number of moveable bodies}) - \text{Number of active constraints} \quad (1)$$

In this mechanical system, we have two moveable parts and two joint presents in each movable part: The revolute joint, Cylindrical Joint. Revolute joint allows one independent motion and its constraints two rotational motions and three translation motions. Cylindrical joint constrains two rotational motions and two translation motions; therefore, it allows one rotational motion and one translation motion.

$$DOF = (6 * 2) - (5 + 4) = 3$$

If the Gruebler Equation of total DOF counts less than zero, it indicated the system has one or more constraints are redundant. In Adams software, the motion applied on body is considered as a constraint. So, it will remove one DOF from the system.

2.4.3.3 Equation of motion - Dynamic Analysis

Equation of motion, a mathematical formula that describes the position, velocity, or acceleration of a body relative to a given frame of reference. A great number and variety of formalisms have been developed for rigid body systems despite the fact that all of them can be derived from a few fundamental principles of mechanics. There are two possibilities to the write equation of motion, either by Newtons force method or Lagrange energy method. Differences between both methods are explained below

(I) Newton's method is based on vector mechanics and on the force (external, inertia etc.) decomposition. Lagrange equations are part of so-called analytical mechanics and it works mainly with scalar quantities like energies.

(II) Newton's laws can include non-conservative forces like friction; however, they must include constraint forces explicitly and are best suited to Cartesian coordinates. Lagrange mechanics is ideal for systems with conservative forces and for bypassing constraint forces in any coordinate system. Dissipative and driven forces can be accounted for by splitting the external forces into a sum of potential and non-potential forces. [15]



(III) For motion calculation, Newtonian mechanics would require solve time-varying constraint force required to keep the body in the constrained motion. For the same problem using Lagrangian mechanics, one looks at the path the body can take and chooses a convenient set of independent generalized coordinate that completely characterizes the possible motion of the particle. This choice eliminates the need for the constraint force to enter into the resultant system of equations. ADAMS uses the Euler-Lagrange to generate Equation of motion for the model. [15]

Let p be a matrix containing the position of all parts in the system i.e. x, y, z Cartesian coordinates and

$$p = [x, y, z]^T \quad (2)$$

In ADAMS, the orientation of the rigid body defined by 3-1-3 (z-x-z) Euler angle and the corresponding angle of rotation of the parts φ, ϕ, θ respectively

$$\epsilon = [\varphi, \phi, \theta]^T \quad (3)$$

The set of a generalized coordinate system associated with a rigid body in ADAMS defined by

$$q = [p, \epsilon]^T \quad (4)$$

The generalized velocity of the body in both longitudinal and angular direction

$$u = \dot{p} \quad (5)$$

$$\omega = B\dot{\epsilon} \quad (6)$$

The generalized acceleration of the body

$$\ddot{q} = [\ddot{x} \ \ddot{y} \ \ddot{z} \ \ddot{\varphi} \ \ddot{\phi} \ \ddot{\theta}]^T \quad (7)$$

It is much more convenient and simpler to use the Lagrange's equation it is shown in below

$$\frac{d}{dt} \left[\left(\frac{\partial L}{\partial \dot{q}} \right)^T \right] - \left(\frac{\partial L}{\partial q} \right)^T + \lambda \Phi_q^T = Q \quad (8)$$



Where

λ – Lagrange multiplier vector

Φ_q – Jacobian of constraint equations

Q – generalized force vector

$$\frac{d}{dt} \left[\left(\frac{\partial L}{\partial u} \right)^T \right] = M \dot{u} \quad (\text{or}) \quad \frac{d}{dt} \left[\left(\frac{\partial L}{\partial \dot{q}} \right)^T \right] = M \ddot{p}$$

$$M = \begin{bmatrix} m^i & 0 & 0 \\ 0 & m^i & 0 \\ 0 & 0 & m^i \end{bmatrix} \text{ - Mass matrix}$$

$$\left(\frac{\partial L}{\partial q} \right) = 0 \quad (9)$$

$$L = T - V \quad (10)$$

$$\text{Total kinetic energy } T = \frac{1}{2} u^T M u + \frac{1}{2} \omega^T J \omega$$

$$\text{Potential energy } V = Mgh$$

$$J = \begin{bmatrix} I_{xx} & -I_{xy} & -I_{xz} \\ -I_{yx} & I_{yy} & -I_{yz} \\ -I_{zx} & -I_{zy} & I_{zz} \end{bmatrix} \text{ - Inertia matrix}$$

Finally, the time variation of the generalized coordinates is related to the translational and angular momentum

$$M\dot{u} + \lambda\Phi_q^T = Q \quad (11)$$

In the above equation, M indicates both masses and inertia matrix and Q indicates all other forces and torques affects the motions. This equation allows the use of scalar quantities such as work, potential energy and kinetic energy instead of vector quantities such as force and acceleration. Moreover, this can be derived from the principle of virtual displacements or extended Hamilton's principle.



2.4.3.4 Constrain equation

Joints in ADAMS are regarded as constraints that act among some of the coordinates. From a mathematical perspective, such a constraint assumes the expression

$$\Phi(q) = 0 \quad (12)$$

The collection of all constraint equations can be written as

$$\Phi(q) = [\Phi_1(q) \ \Phi_2(q) \ \Phi_3(q) \ \dots \ \dots \ \dots \ \Phi_m(q)]^T$$

Where

m – total number of constraints

n – number of generalized coordinates

In order to satisfy ADAMS condition, $m < n$; the number of generalized coordinates is greater than the number of constraints.

In this model we have two dog clutches. One clutch is provided with a revolute joint so, Adams would induce six ordinary differential equations and five algebraic equations to allow one degree of freedom between the two bodies connected by this joint. Second dog clutch is equipped with cylindrical joint, Adams creates six ordinary differential equations and four algebraic equations to allow two DOF between the bodies. Three second-order differential equations in the system govern the motion of the system which must comply with 9 constraint equations.

2.4.3.5 Contact model theory

Contact between objects is an important aspect of multi-body dynamics. It is a discontinuous, non-linear phenomenon and therefore requires iterative calculations. In contact mechanics, the contact force can be calculated either by rigid modelling or using finite element methods. In rigid modelling contact force can be determined by Hertzian contact of general non-linear force formulation using penetration depth and velocity. On the other hand, using the finite element method the contact force is determined by local deformation of the nodes and geometry. The rigid body modelling and Hertzian contact theory were chosen for dog clutch simulation because of the limited number of nodes in the ADAMS student version and because of sufficient accuracy of the rigid model with continuous contact in the case of dog clutch simulations.

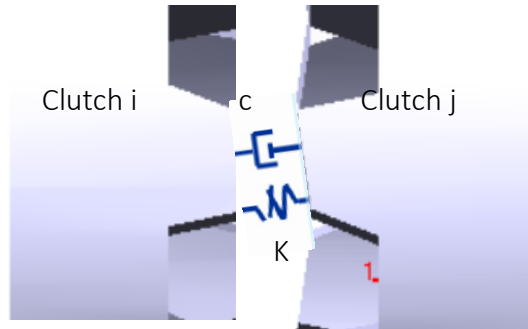


Figure 18 - Dog to Dog contact dynamics

The contact forces consist of two components. One component is in the direction of the common normal and the other component is perpendicular to this normal. The first is called the normal force and the second is called the tangential friction force.

Normal contact force

The contact and impact force consists of two parts that are equivalent to very stiff springs based upon Hertz contact stresses: the elastic force produced by the interaction of the two components, and the damping force produced by the relative motion between two components in contact with each other [16]. The elastic component is a function of penetration between clutches and it opposes the penetration. The damping component of a force is a function of penetration velocity. At the initial contact, the penetration velocity between clutch is high and will leads to higher contact force. Therefore, the damping component is regularized by STEP function and penetration velocity starts from zero.

The normal force vector acting at dog clutch is $F_N^i = [F_{N_x} F_{N_y} F_{N_z}]^T$

The normal contact forces

$$F_N = \begin{cases} K\delta^e - STEP(\delta, 0, 0, d_{max}, C_{max})\dot{\delta} & \delta > 0 \\ 0 & \delta \leq 0 \end{cases} \quad (13)$$

If $\delta > 0$, Penetration occurs between bodies and contact force is greater than zero.

If $\delta \leq 0$, no penetration occurs between bodies and contact force is equal to zero

If, $e = 1$ linear spring-damper model The ADAMS the instantaneous damping coefficient is, a cubic step function of the penetration, given as follow:

$$STEP(\delta, 0, 0, d_{max}, C_{max}) = \begin{cases} 0, & \delta \leq 0 \\ C_{max} \left(\frac{\delta}{d_{max}}\right) \left(3 - 2\frac{\delta}{d_{max}}\right) & 0 < \delta < d_{max} \\ C_{max} & \delta \geq d_{max} \end{cases}$$

Where

K – stiffness of the contact

δ – Penetration depth

e – Contact force exponent – defines force deformation

C_{max} - maximum damping coefficient

d_{max} – penetration depth at maximum damping is applied

Force exponent

The force component makes a linear-spring damper model to nonlinear spring damper model.

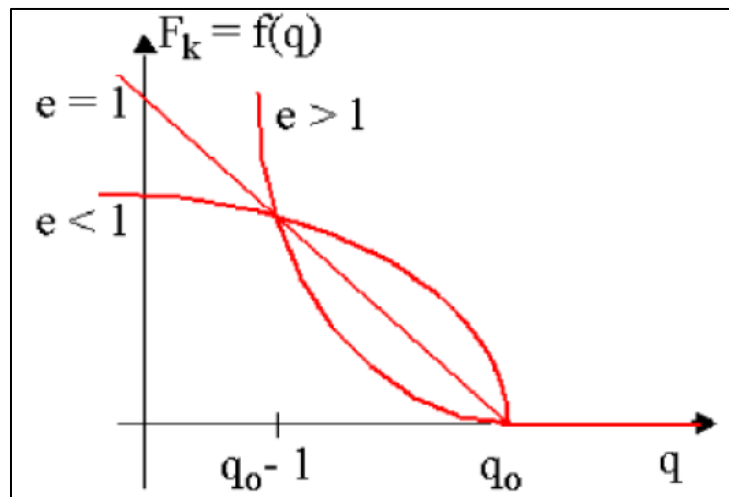


Figure 19 - Shows the behavior of the IMPACT function's spring force and damping force [17, p. 12]

- For $0 < e < 1$, the spring force concaves down and at $\delta = 0$, the slope is infinite.
- For $e = 1$, then system act as a linear spring-damper model and perfectly elastic i.e. no energy loss during the contact
- For $e > 1$, the spring force convex up and at $\delta = 0$, the slope is zero.

Penetration depth

This penetration depth is not the maximum penetration depth, but the measure of how the damping coefficient ramps up from zero to the maximum damping coefficient. To avoid the function discontinuity caused by the dramatic variation of the damping force while contact-collision occurs, the damping force is set to zero when the penetration depth of the two contacted bodies is zero and approaches to a maximum force value when the specified penetration depth d is reached.

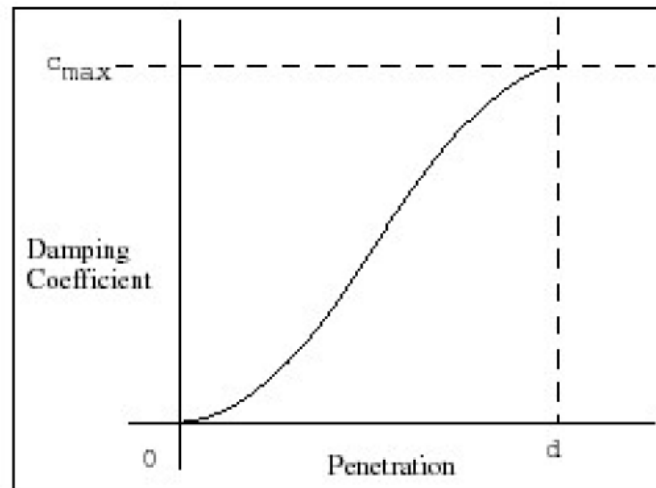


Figure 20 - Damping coefficient vs Penetration [18]

Tangential friction force

The friction problems become more complicated due to the fact the friction law exhibits two phases of behavior. The Coulomb friction law is very useful to predict the friction force. However, Coulomb friction is undetermined when two parts are stick as well as it would produce non-smooth oscillation in the numerical solution due to change of sliding speed direction. To prevent this, the friction model should be refined, and it was done by regularized friction law. In regularized friction law, friction coefficient becomes a function of relative tangential speed and neglecting friction forces in case of zero relative velocity in the friction directions.

In Adams two variable are used to define the regularization: stiction transition velocity and friction transition velocity. The stiction transition velocity defines transition of the coefficient of friction from dynamic to static when the slip velocity equal to the specified value. The friction transition velocity defines transition of the coefficient of friction from static to dynamic when the slip velocity equal to the specified value.

$$0 < \textit{Stiction transition velocity} < \textit{Friction transition velocity}$$

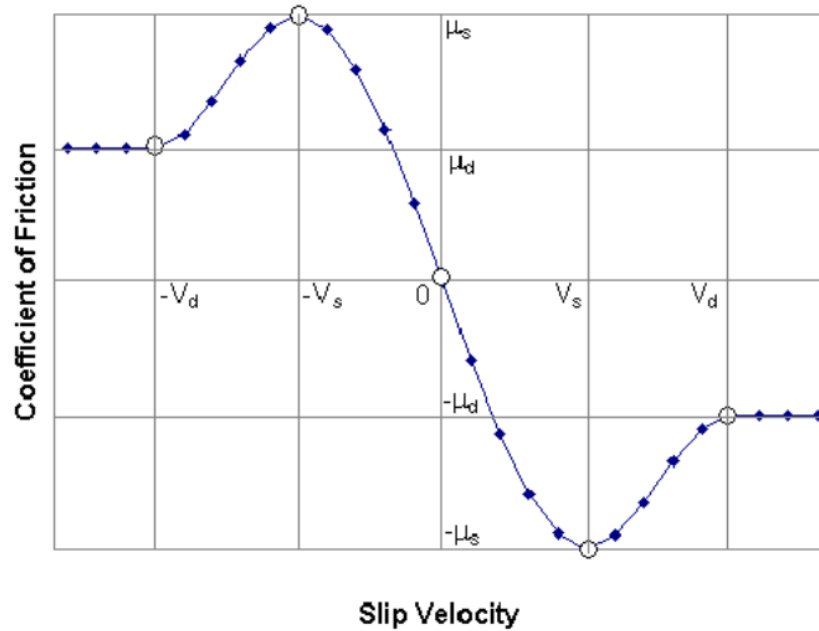


Figure 21- Coefficient of friction Vs slip velocity [19]

The Coulomb friction model in Adams is used for calculating tangential frictional force shown in figure 21

$$\text{The frictional force } F_T = \mu(V_s)F_N \quad (14)$$

Where

$\mu(V_s)$ – Friction coefficient as a function slip velocity vector $V_s = [V_{s\ x} \ V_{s\ y} \ V_{s\ z}]$

2.4.3.6 ADAMS Solving method

- During a simulation, ADAMS/Solver describes the locations and orientations of all mechanical system parts in terms of six coordinates, three translational, and three angular.
- ADAMS/Solver stores time-dependent translational and angular displacements, velocities, and accelerations in the state vector.
- The state vector also contains current values of the reaction and applied forces on each of the parts at the constrained and inertial locations. Thus, the state vector provides a complete description of the mechanical system for a mechanical system simulation.

3. Experiment testing and analysis

3.1 Testing

As already mentioned in chapter 2.2.3, this thesis work is a continuation of the research work of 'Dog clutch with blocking mechanism'. But the whole experiment was conducted without blocking mechanism because the main focus in the experiment was to find engagement time for different input values. Consequently, the simulation also tested without a blocking mechanism.

In the test bench, two main parameters of the dog clutch have taken as input parameter: Gear shifting force and relative angular velocity of dog clutch. The experiments were taken for four different gear shifting force and seven different relative angular velocities. In each case, the experiment was carried out 10 times to measure the average engagement time because of the uncontrolled initial angular position of the dogs.

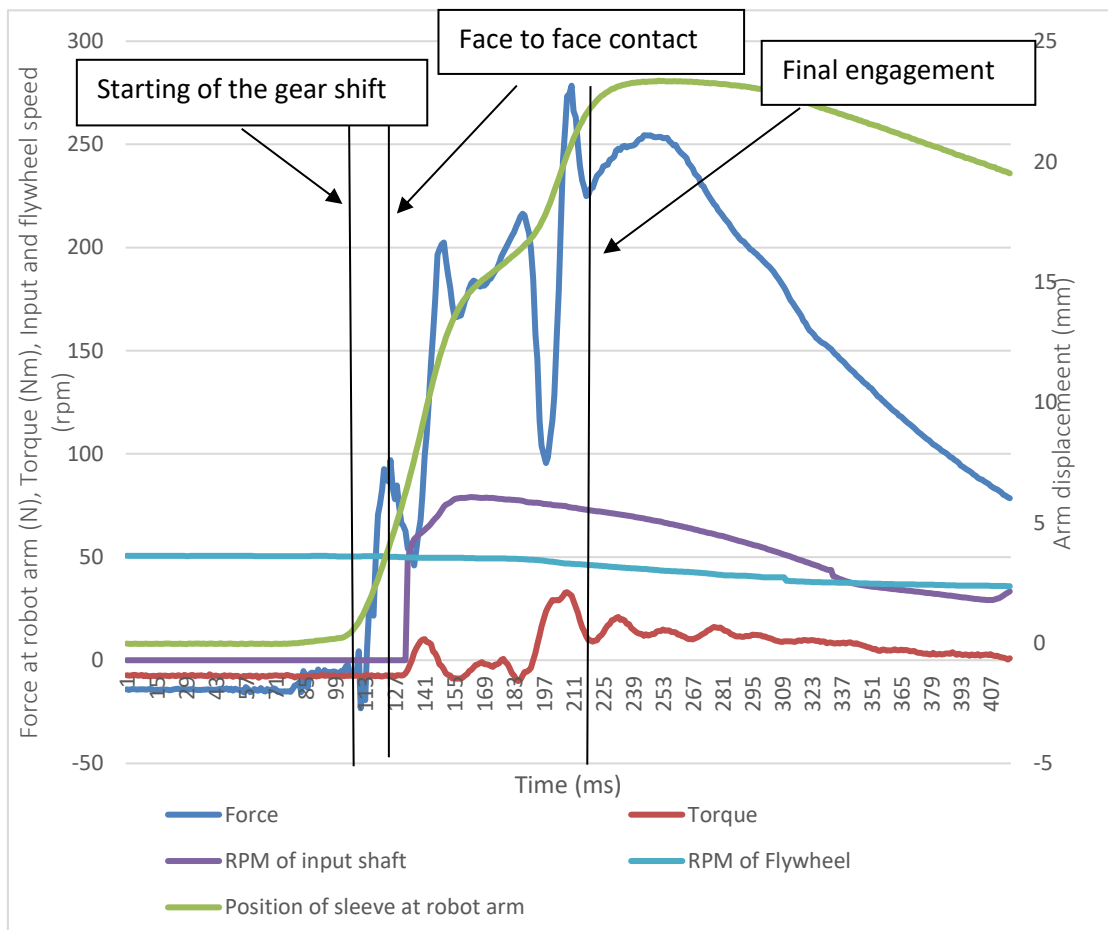


Figure 22 - Test bench measurement with relative angular speed difference of 49.8 rpm and cylinder pressure of 2000 millibar



To explain what is happening inside the gearbox, one of the experiments is explained below. Figure 22 provides the information about the gear shifting process of the dog clutch at the condition of $\Delta\omega = 100 \text{ rpm}$ and gearshift pneumatic cylinder pressure of 2000 millibar. During the testing, the flywheel speed was set to 20 rpm which corresponds to 100 rpm with considering the differential and 3rd gear ratio. The input shaft speed was set to zero rpm, so the relative angular velocity of the shifting is $\Delta\omega = 100 \text{ rpm}$.

The gear shifting process in the experiment differentiated by the gear shift force because the position of the sleeve measure at the robot arm and sometimes it does not provide the intermediate phase changes of the dog clutch engagement. In the beginning, the compressed air supplied to the pneumatic cylinder to increase the pressure in the circuit, consequently shift force also start to increase. The increase of the shift force, in the beginning, used to overcome friction resistance between dog clutch and input shaft and the shifting mechanism. After that sliding dog starts to accelerate and move towards the output dog.

The first face to face contact occurs, the stored translational kinetic energy of the sliding dog exhausted and this sudden impact reduces the shifting force. Due to the different angular velocities, causes the dogs to slip each other and the angular kinetic energy of the sliding dog starts to increase gradually.

The final engagement occurs once the sliding dog reaches the slot of the output dog clutch. When the dogs go through the slots, still there are relative speed difference presents which causes the sudden increase of the torque value. After the engagement sliding and output dogs are starts to rotation at same speed.

3.2 Analysis

The measured data from the test bench should be analysis to get useful information and then the collected information integrated with simulation to run the simulation as close as to the experiment. The measured values from the sensors were collected by the NI LabVIEW and it creates a different set of files for each shifting.

3.2.1 Gear shifting force

The gear shifting in the gearbox is carried out using a pneumatic shifting robot. A gear shift robot arm connected to the six pneumatic cylinders to control the gear shift lever mechanism by two cables. The pressure of the air flowing into the cylinders is controlled by a pressure relief valve which allows the different shifting force for different cases.

The gear shifting force measured in the outside of the gearbox at the robot arm and the force value is not constant which changes according to the cylinder pressure. But in simulation gearshift force directly applied on the shift sleeve and to calculate shifting force at the shift sleeve, linkage ratio was defined. Linkage ratio defined as the ratio of robot arm displacement to simulation sleeve displacement. This linkage ratio differs for the different pressure value and the reason behind is that material compression starts to increase when the pressure in a pneumatic circuit increase and it makes difficulties to calculate the linkage ratio.

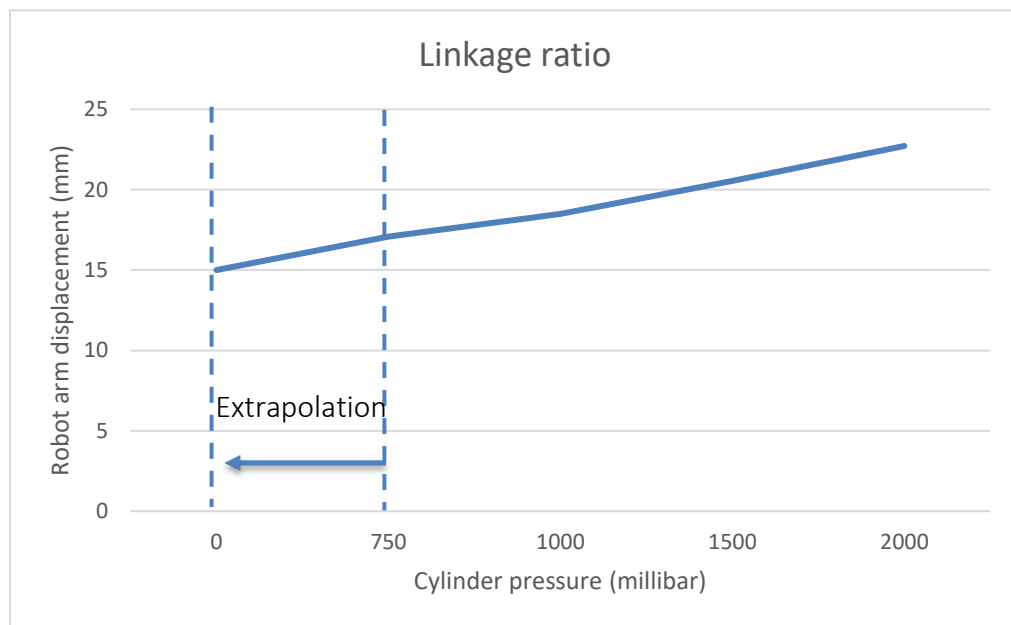


Figure 23 - Linkage ratio

To avoid the multiple linkage ratio, we used the extrapolation method to get better linkage ratio value. However, the error (or) uncertainty increase when extrapolation is used for long-range. The efficiency with which gearshift force is transmitted must also be taken into account and it is taken as an 80%



Cylinder pressure (millibar)	Robot arm displacement (mm)	Max force time (s)	Avg force at robot arm (N)	Linkage ratio	Linkage efficiency (%)	Force at sleeve (N)
750	17.0751	0.2510	92.1172	3.1914	80	235.1929
1000	18.4837	0.2026	123.5824	3.1914	80	315.5295
1500	20.5453	0.1766	183.7092	3.1914	80	469.0449
2000	22.7159	0.12614	251.2455	3.1914	80	641.4778

Table 2 - Gearshift force at sleeve

3.2.2 Inertia calculation

The inertia of the output side is calculated from the flywheel inertia and gear ratio of the 3rd gear and differential ratio. The moment of inertia is reduced onto the output shaft. In this case, following reduced moment of inertia applies to the dog clutch of the gear to be shifted

$$J_{red} = J_{out} * i_3^2 * i_{diff}^2$$

From this equation output dog inertia = 0.6048 Kg.m²

Inertia of the input dog = 0.01 Kg.m²

3.3.3 Relative angular velocity

In the test bench gearbox, the sliding dog is in the state of free rotation and does not rotate until it contacts with output dog clutch. The output dog clutch rotates with the help of AC synchronous motor, which is coupled with inertial flywheel.

$$\text{Angular velocity difference } \omega_{rel} = \omega_1 - \omega_2$$

Where

ω_2 – Output dog clutch

ω_1 - Sliding dog clutch



Flywheel RPM	Overall ratio $i_3 * i_{diff}$	Relative angular velocity $\Delta\omega_{rel}$ (rpm)
1	4.98	4.98
2	4.98	9.96
5	4.98	24.9
10	4.98	49.8
20	4.98	99.6
30	4.98	149.4
50	4.98	249

Table 3 - Relative angular velocity (rpm)

3.3.4 Experiment result

The dog clutch in gearbox shifted from natural to 3_{rd} gear for 25 times with different shift force and relative angular velocity. To find the average engagement time, each experiment data was analyzed.

		Force [N]				
		235.2	315.5	469.0	641.5	
RPM difference [1/min]	5	0.4807	X	X	X	Time (s)
	10	0.3318	0.3807	0.2688	0.1764	
	25	0.2079	0.2062	0.1803	0.1394	
	50	0.1983	0.1905	0.1588	0.137	
	100	0.2064	0.1764	0.1559	0.1364	
	149	0.197	0.1799	0.1546	0.1393	
	249	0.1956	0.1712	0.1504	0.1363	

Table 4 - Average engagement time in experiment



4. Dog clutch modeling and simulation

4.1 Creating MBD model

Basic step by step procedures needed to accomplish the analysis of a gear shifting in MSC ADAMS are introduced below

Build a Model .CADPart

- Create physical bodies including exact geometrical shapes such as length, width, dimension, and distance between dog clutches etc.

Build a ADAMS .bin

- Apply physical characteristics such as mass, principal mass moment of inertia and friction coefficients.
- Fulfil the kinematics definitions such as translation and rotation.
- Simulation that relates to making the motion, forces and observing model behavior

Review .biq

- Record and analyses result in the MSC ADAMS Postprocessing

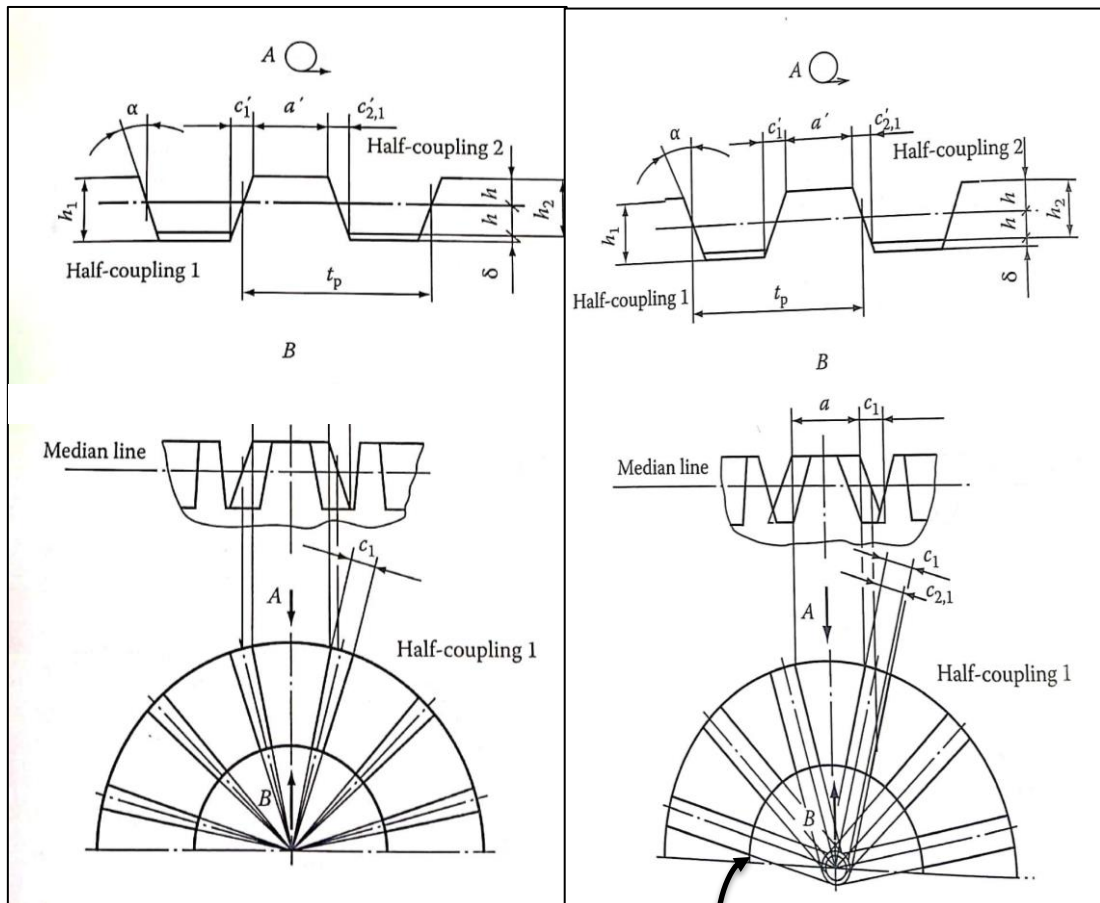
4.1.1 Geometry of the trapezoidal dog

The geometrical model has to be carried out by 3D modelling software such as Pro-E, Solid Work and CATIA. The last software was chosen to model the dog clutches. The dog designs are modelled in Catia V5 based on the experimental setup dog clutch with parameterization.

The drawing of the trapezoidal dog 3D model is complex compared to the rectangular dog because the trapezoidal dog does not follow the rectangular dog design principle. The rectangular profiled dog is designed by drawing rays from their common axis of center and during the engagement, the contact surface of the rectangular dog coincides each other and transmit the torque.

If the trapezoidal dog follows the standard design procedure, then dog clutch engagement would not be succeeded and Instead of face to face to contact, face to edge starts to contact. The main reason for this, the nonequal contact surface and this

are shown in figure 24(a). The lateral skewed surfaces of adjoining dogs cannot contact over the entire surface since their outer edges move apart when approaching the center from the periphery. In the best case they may contact along a line and in a worst-case, along with individual points. However, in both case clutch cannot operate. The working surface of the correctly designed dog look like parallelograms and conversely, when the dog was not properly designed, as nonequilateral trapezes. [7]



Identical height of the dogs

Figure 24 - (a) Incorrect and (b) correct geometry of trapezoidal dog [7, pp. 247-248]

The tested trapezoidal dog clutch in the experiment consists of positive side angles with the chamfered face. The center line lies on a median plane that divides the height of the dogs in halves. To design proper working trapezoidal dog insertion of the slope surfaces of its dog form of lateral plane. This lateral plane produces an identical height of dogs over their entire length, it is shown in figure 24 (b). The intersection of the lateral plane of the dog and median plane results, that a line in a point goes to the center of the dog geometry. The design parameters are listed below in table 5

Parameter	Value
Number of dogs	15
Angle of traction side contact surface	12°
Angle of braking side contact surface	22°
Angle of chamfered face	8°
Dog height	3.7 mm
Outer diameter	52 mm
Inner diameter	44 mm

Table 5 - Dog design parameters

4.1.1.1 Reason for side angles

The minimum angle of traction and braking side contact surface are depending on the self-locking angle. The self-locking depends on the coefficient of friction of the material and side (or) cone angle. To prevent the dogs from self-locking, the following equation must apply for the side angles α

$$\tan \alpha > \mu$$

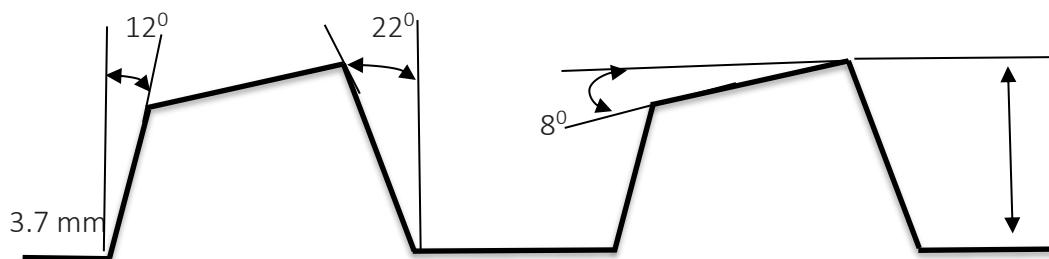


Figure 25 – Geometry of trapezoidal dog

The static coefficient of friction depends on the material of the dog clutches and lubrication between. Dynamic friction is lower than static friction and correspondingly, dynamic self-locking is less likely to occur than static self-locking [20]. The trapezoidal dog tested was asymmetric shape so, it cannot transfer the same amount of torque in both sides and it is explained in the chapter 2.1.6 Conversely, the large-angle provides better engagement, but axial force generated during torque transmission is increased.

4.1.1.2 Reason for chamfered face

The chamfered face angle is providing better dog clutch engagement and reduce the friction phase sometimes it will eliminate the friction phase that depends on the relative angular velocity. The optimal engagement time can be determined by the chamfered angle. In the rectangular dog, there is a possibility of dogs are stuck at face to face contact due to the low relative angular velocity. If the faces are chamfered the engagement is successful even at low relative speed difference. The tested dog clutch has chamfer of $\beta=8^\circ$.

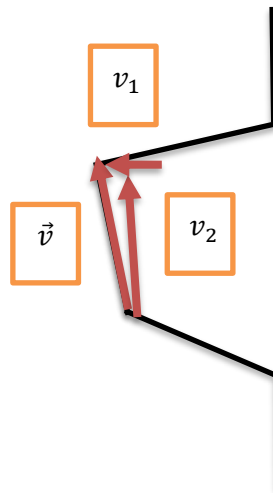


Figure 26 - Velocity vector at dog

$$\text{Horizontal component } v_1 = \frac{\text{Displacement}}{\text{time}} = 17.07509 \text{ mm/s}$$

From the chamfered angle $\tan \beta = \frac{v_1}{v_2}$ we can find v_2 by applying v_1 in this equation

$$\text{Vertical component } v_2 = 121.53 \text{ mm/s}$$

The equation for dog clutch tangential velocity at middle of the dog is written as

$$v_2 = \Delta\omega * \text{dog radius at the middle}$$

$$\text{Dog radius at the middle} = 56 \text{ mm}$$

$$\Delta\omega = 130 \text{ RPM}$$



The above calculated relative angular velocity gives optimal engagement time, meaning at this value of $\Delta\omega$ eliminate the face to face contact instead of that side faces starts to contact.

4.1.1.3 CATIA

Inside CATIA, the first step is to sketch a 2D drawing of the dog clutch with parameterization which will help for modifying the 3D geometrical model automatically. This is converted into the 3D model. The dog clutch used for the experiment is new, therefore unnecessary geometry such as fillets and chamfers are not used in the 3D model.

The 3D model saved as default CATIA file format (.CADPart) that could be imported directly into ADAMS as a solid. There is no need to convert into an intermediate file format like Step files (.stp/.step), Iges, Parasolid. The main advantage of taking as solid is, if density is applied in the geometry then ADAMS could automatically calculate center of mass, mass, and rotational inertia of the parts.

4.1.2 ADAMS model

The coordinate system in the MSC Adams model was set equal to the coordinate system used in a Catia CAD model. We are using forward dynamic principle to calculate the engagement time because the shift force is one of the main input parameters and is affecting the motion of the dog clutches.

When the dog clutch model is imported with the above method, each component comes inside the ADAMS and still have no connection between one another. Following chapter will describe the procedure to get a realistic virtual model in ADAMS.

4.1.2.1 Mass and inertia properties

To solve the equations of motion in rigid modelling, Adams required some mechanical properties like mass, mass moments of inertia, gear shifting force and motion. To get more accurate mass and inertia properties of the dog clutches in the model, these values are directly measured from the experimental setup and implemented in ADAMS. Mass and moment of inertia with respect to the local coordinate system are listed in below table

Sliding (or) input dog clutch	Mass (Kg)	I_{xx} (Kg.m ²)	I_{yy} (Kg.m ²)	I_{zz} (Kg.m ²)	
	0.3		0.01	0	0
			0	0.005	0
		0	0	0.005	
output dog clutch	Mass (Kg)	I_{xx} (Kg.m ²)	I_{yy} (Kg.m ²)	I_{zz} (Kg.m ²)	
	1		0.6048	0	0
			0	0.3024	0
		0	0	0.3024	

Table 6 - Mass and Principle mass moment of inertia

4.1.2.2 Joints and constraints

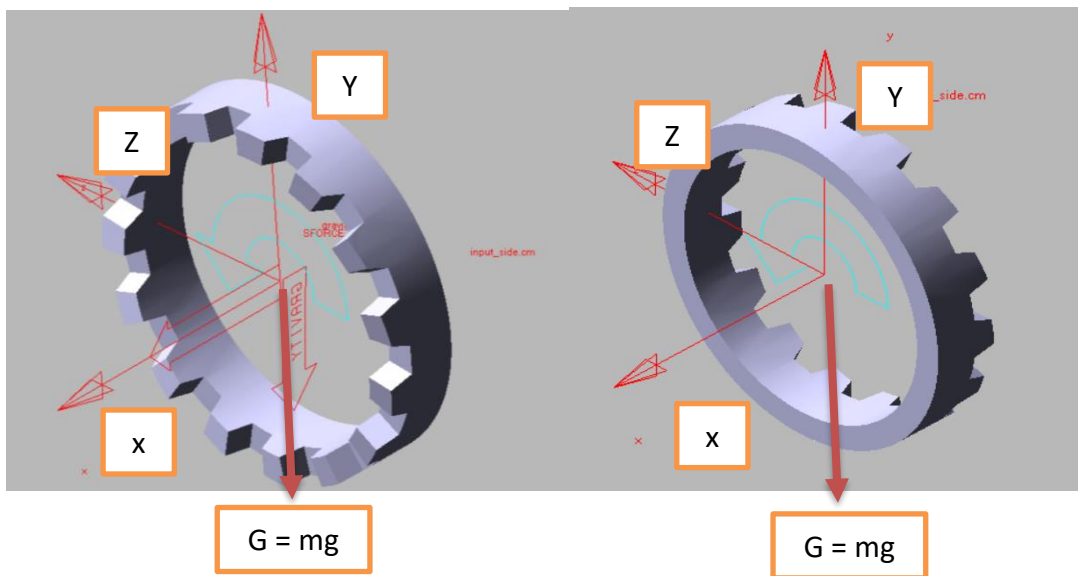


Figure 27 – Scheme of dog clutch in ADAMS

(a) sliding dog

(b) output dog

The sliding dog and output dog scheme are shown in Figure 27 with respect to the local body coordinate system. The revolute joint is added to the output dog (b), so that it can rotate around its own axis. The orientation of the body coordinate system vector with respect to the global coordinate system $\Phi^1(q) = [x \ y \ z \ \phi \ \theta]^T$ at any time is equal to the initial orientation at $t = 0$. Similarly, the cylindrical joint is applied on the (a) sliding dog (a)(a)(a), $\Phi^2(q) = [y \ z \ \phi \ \theta]^T$ does not change with time.

4.1.2.3 Gear shifting force

In the simulation, shift force is acting on the sleeve. At the start of the shift operation, the shift force is simulated by a polynomial approximation STEP function using the independent variable of TIME.

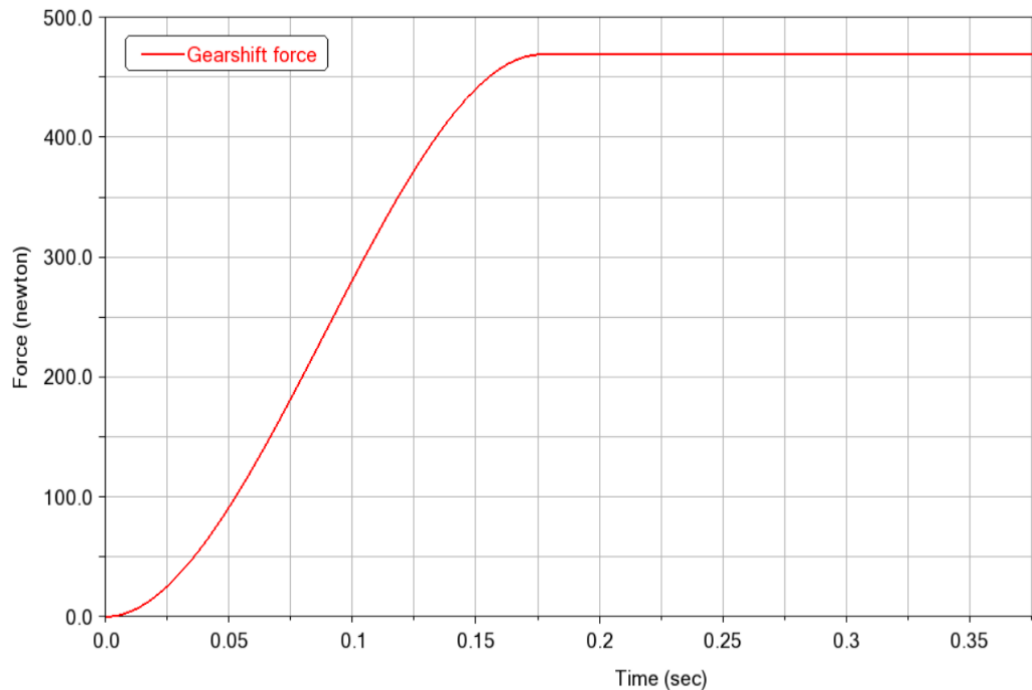
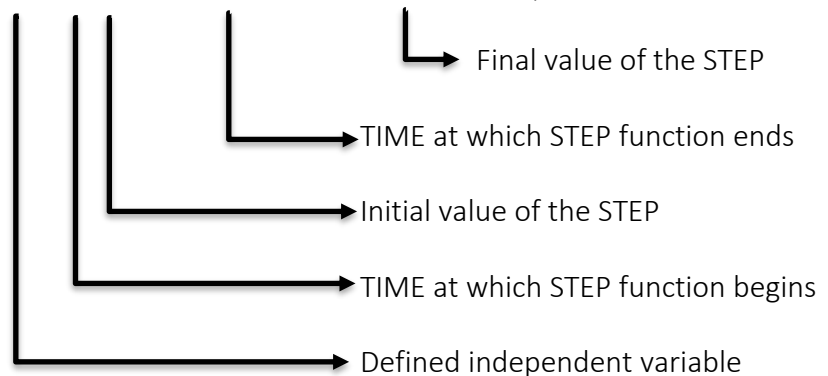


Figure 28 - Gearshift force at $\Delta\omega = 100$ rpm, $F_{max}=469$ N

Force = STEP (TIME, 0, 0, Max force time Force at sleeve)



4.1.2.4 Geometrical Contact

The bodies in ADAMS do not by default notice a collision during the simulation. The contact function is applied to the specific parts where the collision occurs. The corresponding contact function is activated when the distance between two dog clutches becomes negative. In this model, when two half-clutches encounter each other, and a nonlinear contact characteristic is introduced to determine the contact force and friction force. In chapter 2.4.3.5 explained about contact theory and equation.

To determine the realistic contact parameters (i.e. stiffness, damping, static, dynamic coefficient and penetration depth), the systematic design of experiment approach was applied in the MBD model. The values of these parameters cannot be estimated precisely due to the availability of data and complexity of contact shapes.

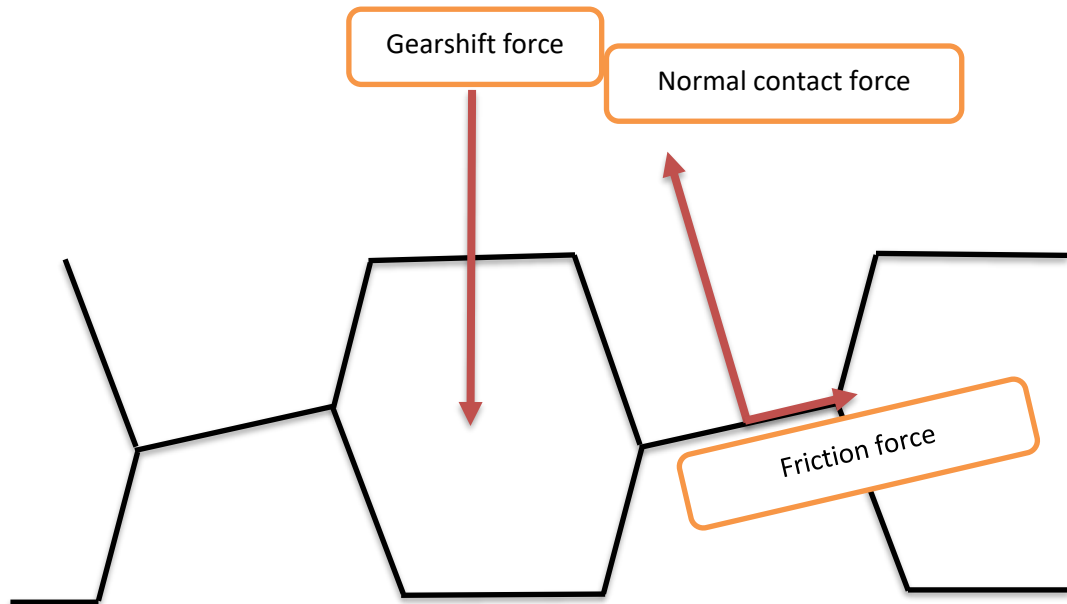


Figure 29 - Normal contact force and tangential friction force

4.2 Sensitivity analysis of the parameters influence

A mathematical model can be highly complex, and its relationship between inputs and outputs may be poorly understood. So, to get realistic model for complicated simulations two analysis are involved: Uncertainty and sensitivity analysis.

The sensitivity analysis investigates the relationship between input parameters and output of a simulation model. A sensitive analysis is done to see how material stiffness, damping and coefficient of friction, affect the dog clutch engagement time in the simulation. The sensitive analysis is done by either Design of study (or) Design of Experiment.

4.2.1 Design study (or) one-way sensitivity analysis

Design study, which examines the effects of changing the parameter by considering one parameter at a time. Using a study design analysis, we can determine how the output varies with changing the parameter and optimal value can be determined among the simulated values.



4.2.2 Design of Experiment (or) two-way sensitivity analysis

DOE which is used to change two or more parameters at a time while the design of study changes only one parameter at a time. When analysis is a process, experiments are often used to evaluate which process inputs have a significant impact on the process output and it improves the reliability of the model. DOE in Adams using the full factorial method. In full factorials, all the possible combinations that are associated with the factors and their levels are studied.

$$DOE_{trail} = x^y$$

Where

x – number of runs

y – number of parameters to change

4.2.3 Stiffness coefficient K

The stiffness of the contact model depends on the young's modulus and Poisson's ratio. Even though the name stiffness might sound like it is a material property, it is not just that. It also depends on the geometry of the colliding objects. Therefore, there is no handbook for choosing the value for stiffness. The best option is to do multiple simulations in Adams with different values of stiffness to determine the optimal value, the value at which the Adams contact behavior resembles the real-world contact behavior. [17]

4.2.3 Damping coefficient C_{max}

Energy loss during the collision is usually modeled as a damping force that is specified with a damping coefficient. Based on the research papers in gearboxes, the damping coefficient generally takes values 0.1%~1% of the stiffness K. In ADAMS, the standard value of the stiffness coefficient is $1 \cdot 10^8$ N/m and maximum damping coefficient is $1 \cdot 10^4$ N-s/m, which is 0.01 % of the stiffness value. The optimal value of the damping coefficient can be determined by DOE which resembles the real-world contact behavior.

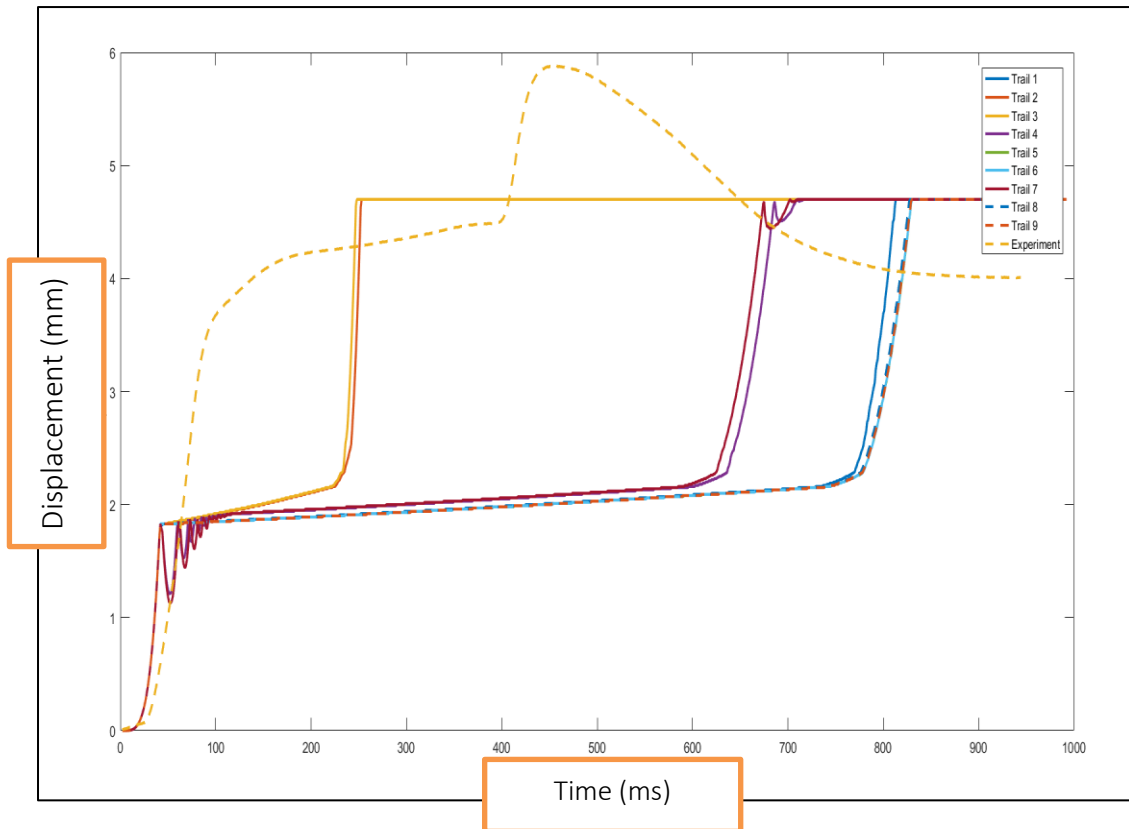


Figure 30 - DOE result for Stiffness and Damping compared with experiment

To get the optimal value, the DOE result should be correlated with the experiment but due to uncertainty's in the test bench DOE results are not comparable with the experiment as shown in Figure 30. It is possible to avoid uncertainty either by redesign the test bench or integrate the experimental shifting mechanism in the simulation model. Either way, it will take more time.

Due to the lack of time, some simplifications were made in the way to run the simulation as close as to experimental setup. The dog clutch used for the experiment is made of steel alloy material (16MnCr5) and density of the 16MnCr5 is 7800 Kg/m^3 [21]. The steel material density is 8000 Kg/m^3 . There is not much difference in density so, we consider steel material as a dog clutch material for simplification. In ADAMS help manual provides the steel material stiffness, damping and friction coefficient values. These values are used for simulation to get the results as real as possible.



The force exponent value taken as 1.5 to get better numerical convergence and computation speed.

Stiffness coefficient (K), N/m	Damping coefficient (C), Ns/m	Force element (e)	Penetration depth (δ), m
$1 * 10^8$	$1 * 10^4$	1.5	$1 * 10^{-5}$

Table 7 - Contact force parameter used for simulation

Static friction coefficient (μ_s)	Dynamic friction coefficient (μ_s)	Static transition velocity (V_s), m/s	Dynamic transition velocity (V_d), m/s
0.30	0.16	0.1	1

Table 8 - Friction force parameter used for simulation

The stiction and dynamic transition velocity DOE results are attached in the “Appendix”

4.3 Solver for nonlinear contact dynamic simulation

Modern methods for the dynamic analysis of constrained multibody systems fall into two main categories: differential-algebraic equations (DAEs) and ordinary differential equations (ODEs). Both are used to obtain the motion trajectories of the rigid bodies given the inertial properties and the non-contact external loads DAEs employ a maximal set of variables to describe the motion of the system and use multipliers to consider the constraint forces. Premultiplying the constraint reaction-induced dynamic equations by the orthogonal complement matrix to the constraint Jacobian results in the governing equations as ODEs. [14]

Unlike kinematic and static simulations, which involve the solution of only algebraic equations, dynamic simulations are more complex because they involve the solution of differential and algebraic equations (DAEs).

4.3.1 Integrator and formulation index

ADAMS/Solver uses linear multi-step integration methods that contain a predictor and a corrector. In ADAMS four stiff integrators and one non-stiff integrator are currently available. The four stiff integrators are: GSTIFF, WSTIFF, constant BDF and RKF45. The non-stiff integrator is Adams–Bashforth–Adams–Moulton (ABAM).



For gear shifting simulation, I have chosen the Gear Stiff integrator (GSTIFF) which gives the best results and is the most robust. It provides good solutions for simulations of stiff models. The method uses a backwards differentiation formula (BDF) to integrate differential and algebraic standard index-three equations.

The index of a DAE is defined as the number of time derivatives required to convert a set of DAEs to ODEs. The Euler-Lagrange equations for mechanical systems are said to have an Index=3. The first two-time derivative converts kinematic position constraint into acceleration kinematic constraint equation. By taking a third and last time derivative of the Lagrange multiplier, only left with a set of ODE equation in acceleration and the Lagrange multipliers.

4.3.2 Error and time step

Error is the difference between the exact solution $f(t)$ and the approximate solution $p(t)$. But in reality, during numerical solution we do not know the exact solution and thus errors are calculated between two successive steps of the numerical solution. Error tolerance is the maximum error allowed per integration step and it can be displacement (or) velocities states.

$$\text{Absolute error tolerance} = |f(t) - p(t)| \quad (15)$$

$$\text{Relative error tolerance} = \frac{\text{Absolute error tolerance}}{|f(t)|} \quad (16)$$

If error is in displacement state, then error has unit of length. From the equation (15), we can say absolute tolerances take the physical dimension of the state and the relative tolerances are dimensionless. Small tolerance values usually result in more accurate results, but the computation effort will be higher. Extremely fine tolerances do not make sense because the influence of numerical rounding and cancellation errors would become too large. Large tolerance values often speed up the calculation, however at the expense of result accuracy. State value changes below the tolerances will not be considered by the integrator.

The integration process depends on how the non-linear equation solved in the time domain. Fixed step-size integrators use the same integration step-size throughout the whole integration. They do not provide any error control and step-size should be small enough to cover all change in dynamics (or) eigen frequencies. The variable step-size integrators use sophisticated strategies to control the integration step-size.

Solver parameter	Value	Reason
Error tolerance	$1 \cdot 10^{-6}$	Gives accurate results
Maximum time step	$1 \cdot 10^{-4}$	To get better convergence
Corrector	Original	It considers error in all solution variable
Newton–Raphson iterations	6	To reduce round-off error

Table 9 - ADAMS used Solver parameters

4.4 Simulation results

The simulation was carried out 10 times for each case to find average engagement time, same as an experiment. For each simulation sliding dog orientation angle was changed around a rotational axis and this angle was randomly created by MS excel command (RANDBETWEEN). The random angles are 37, 91, 114, 148, 196, 216, 232, 258, 313 and 326 degrees. ADAMS is using the 3-1-3 (Z-Y-Z) Euler angle to describe the orientation with a fixed global coordinate system. So, changing the orientation by applying the random angle value at the place of 3 (or) Z.

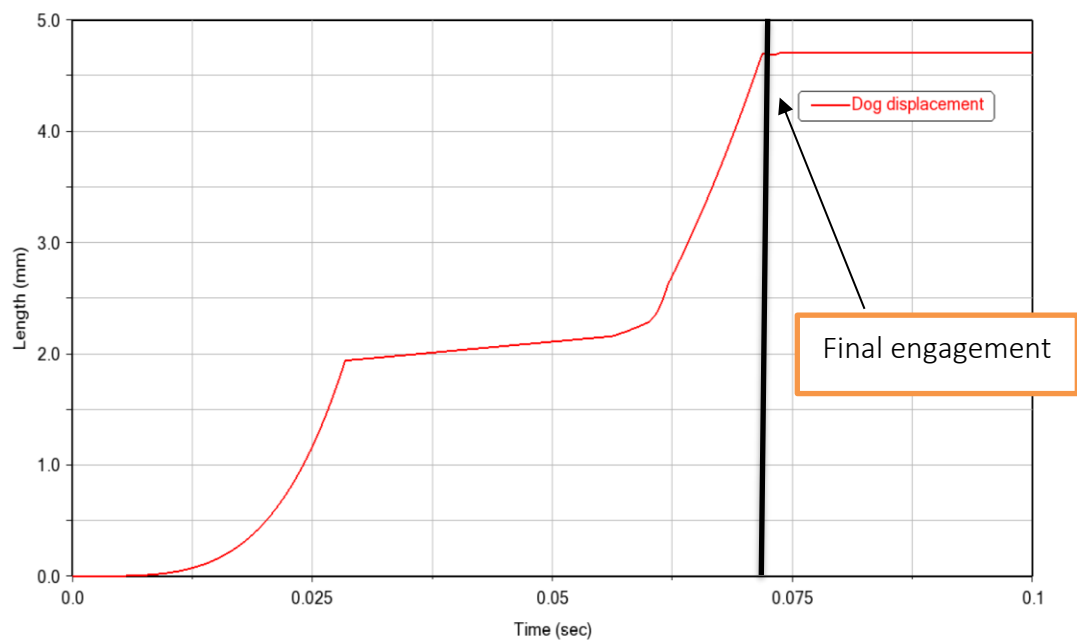


Figure 31 - Simulation measurement with $\Delta\omega = 24.9$ rpm, sliding dog angle $= 37^\circ$ and $F = 235$ N



In the simulation, three parameters of the dog clutch considered as an input parameter: gear shifting force, angular velocity difference and sliding dog angle. For each case, gear shifting force and angular velocity difference kept as constant and sliding dog angle keep on change this represents the uncontrolled initial angular position of the dogs. Therefore, sliding dog angles give different engagement place results in different engagement time. Finally, average engagement time calculated by taking the average of different engagement time.

		Force [N]				
		235.2	315.5	469.0	641.5	
RPM difference [1/min]	5	0.18384	X	X	X	Time (s)
	10	0.14912	0.14267	0.13703	0.12951	
	25	0.09844	0.10266	0.10629	0.09165	
	50	0.07013	0.0617	0.05553	0.05586	
	100	0.07047	0.05974	0.0489	0.0405	
	149	0.06814	0.05727	0.04839	0.03872	
	249	0.067867	0.05761	0.04781	0.03678	

Table 10 - Average engagement time in simulation

5. Dog clutch model validation

The validation process used to determine whether the simulation model accurately represents the real system. So, this chapter deals with the validation of the dog clutch dynamic simulation model by comparing with the experimental result.

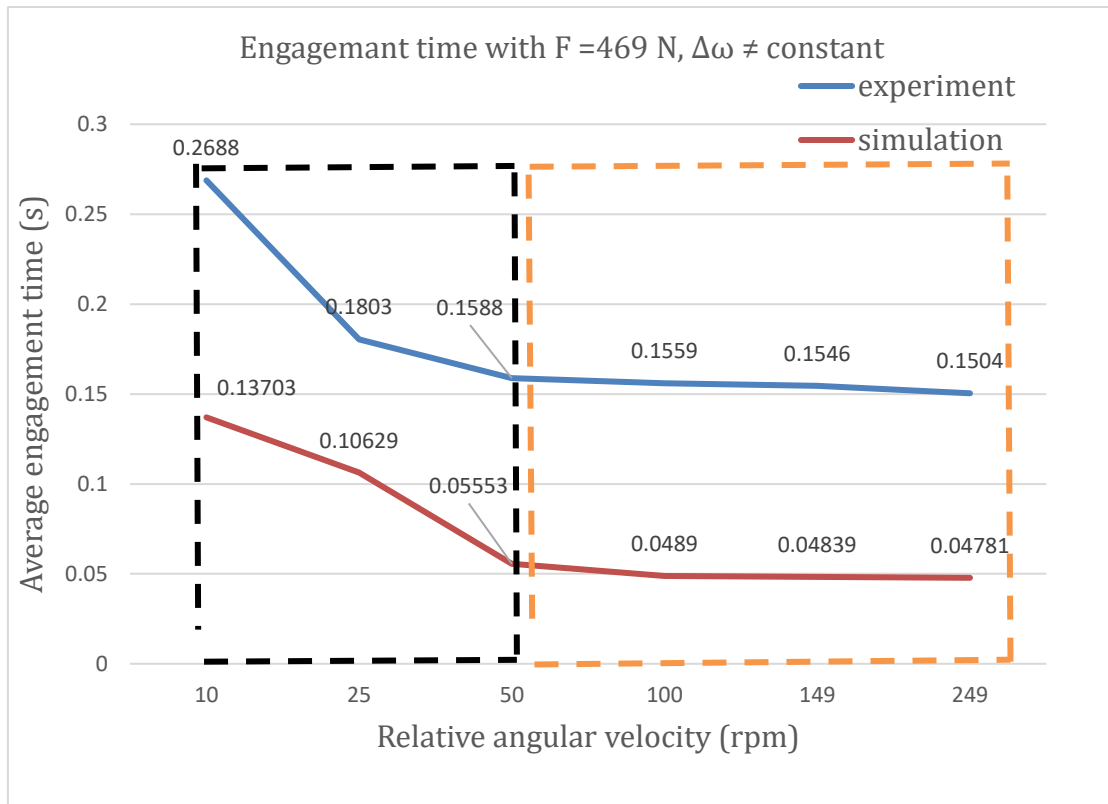


Figure 32 - Average engagement time $F=469\text{ N}$, $\Delta\omega \neq \text{constant}$

Figure 32 shows the comparison between simulation results and experimental results with different relative angular velocity and it can be clearly seen that, there is some time difference in simulation and experiment engagement and the reasons are listed below.

5.1 Reason for lower average engagement time in simulation

5.1.1 From the viewpoint of experiment

(I) The positioning of the sleeve is measured by robot arm, so the measured value of the displacement does not correspond to the actual displacement of the sleeve and robot arm displacement. It depends on the clearance between dog clutch and on elastic deformation of the robot arm material.

In the experiment even after the final engagement, robot arm continues to push the dog clutch and it is clearly seen in Figure 22. This continues force on the robot arm leads to elastic deformation in the components and therefore sensor sense high displacement in the robot arm. The elastic deformation depends on the pressure in the pneumatic circuit. In figure 33 shows the difference between the robot arm and simulation displacement.

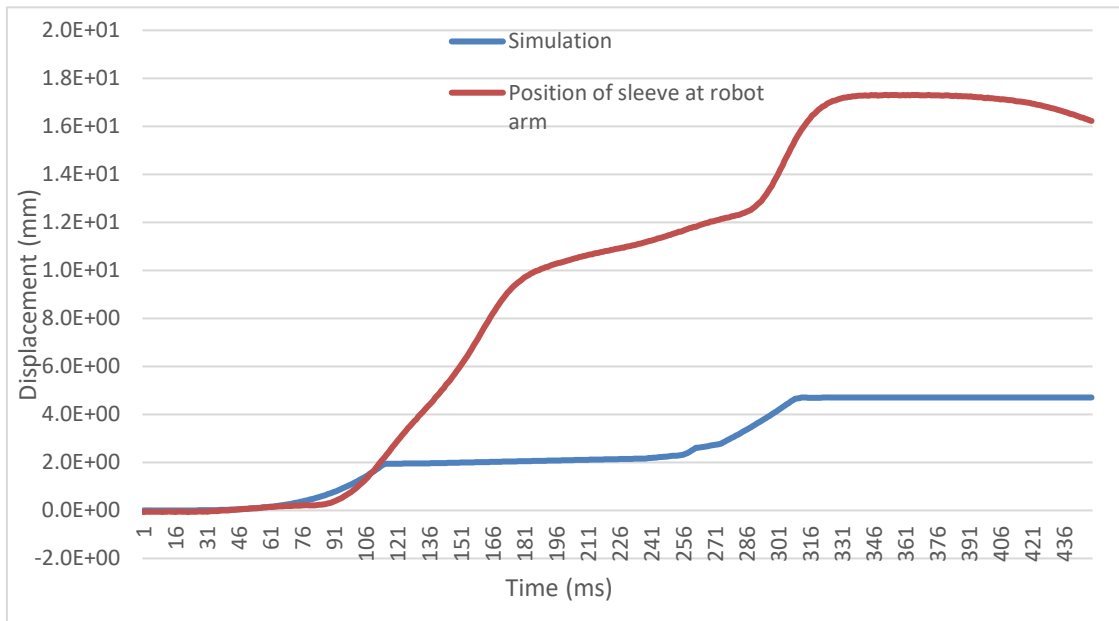


Figure 33 - Displacement of robot arm and simulation

(II) Similarly, the shifting force is also measured in the robot arm and it does not reflect the actual force in the sleeve. The shifting force is not constant and non-smooth in the experiment because applied force changes with respect to the place of engagement.

(III) To obtain displacement and force at sleeve, linkage ratio was defined, and it is determined by the extrapolation method. The extrapolation method produces error (or) uncertainty and the magnitude of an error depends on the range of extrapolation. If the magnitude of error increases, then calculated displacement and force at sleeve values are not comparable with simulation.

(IV) In the experiment the angular displacement of the dog clutch was uncontrollable. Therefore, the place of engagement cannot be defined. The possibility of face to face contact is increased when the relative angular velocity is low. From this point we can say the average engagement time is increased in the case of low relative

angular velocity and it is shown in Figure 32. Once the relative angular velocity increase then there would not face to face contact instead of that face to slot (or) torque transmission side faces starts to contact. So, the uncontrolled engagement mainly considered in the low relative angular velocity.

5.1.2 From the viewpoint of simulation

(I) For simulation simplification, the dog clutch model is considered as a rigid model but in reality, there would be elastic deformation.

(II) The gear shifting force in simulation is defined by polynomial STEP function so, the change of force is smooth but, in the experiment, shifting force is non-smooth and it changes when contact with dog clutch.

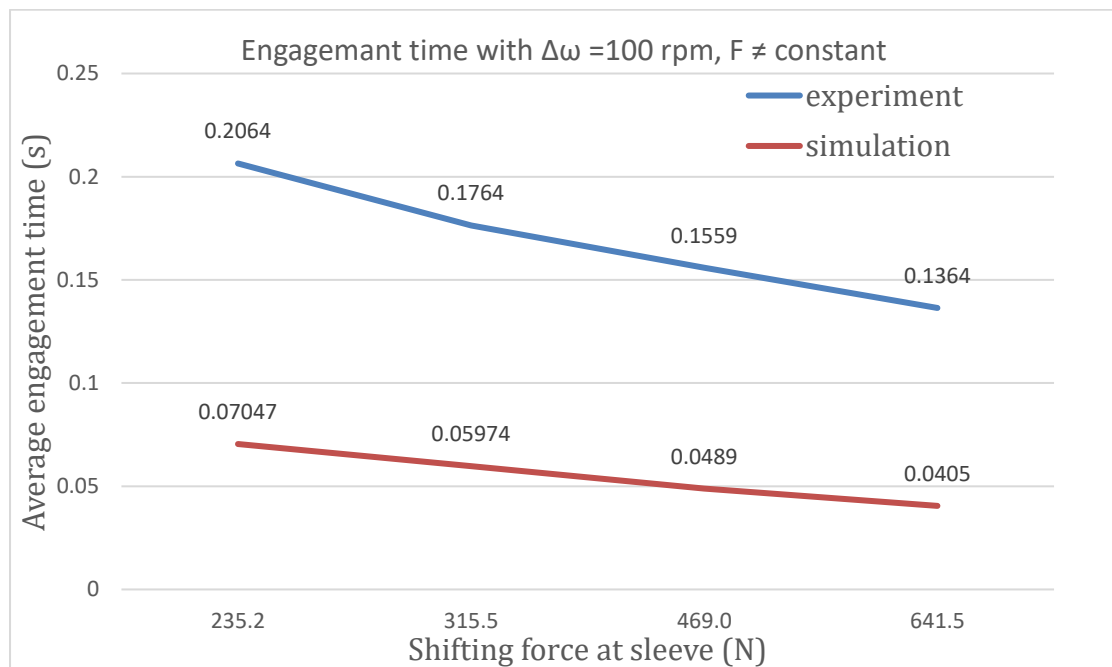


Figure 34 - Average engagement time $\Delta\omega=100$ rpm, $F\neq$ constant

(III) The ADAMS contact parameters such as stiffness, damping, and friction coefficients are not determined by Design of experiment instead of that some reasonable values took from the reference paper and the ADAMS help manual. This will lead to inaccuracy during the simulation.



(IV) The friction between the input shaft and sliding dogs are not integrated into the simulation model and this cause faster engagement in simulation compared to the experiment.

(V) The simulation was carried out for 10 random angles to get average engagement time. The random angles give inaccuracy of result, same as point (IV).

In this chapter 5. only two validation results are attached, and all the other comparisons results are listed in "Appendix".

5.2 Future work

In test bench displacement and force are measured outside the gearbox and this measurement place raising uncertainty. This can be avoided either by measuring inside the gearbox or integrating gear shift mechanism in simulation. I would prefer to go with the second option because we do not need to repeat the experiment once again. However, this integration would be very complicated, and it would be hard to validate it. We are currently working on a new test bench which would measure the force, torque and displacement much closer to the tested gearshift mechanism. Then we hope to be able to carry out more precise experiments to have better comparison with simulation.

Future work mainly concerns on changing the simulation model that will work in a similar way to the experimental setup. For instance, integrating the experimental gear shifting mechanism inside the simulation makes easy to compare the results. On the other hand, it will increase the number of compounds in a simulation model and we have to define each component geometrical parameter such as stiffness and damping coefficients. Anyhow, it will provide the information that can be directly compared with the experimental result. Furthermore, this will hopefully eliminate taking values from research papers.

It could be interesting to consider the friction between the input shaft and the dog clutch. Just applying small negative force on the sliding dog will represent the friction on the sliding dog.

In this diploma thesis all the simulations were carried out as rigid modeling, maybe in the future try to do the simulation with flexible modeling because a flexible body makes the simulation process more realistic than a rigid body.



6. Conclusion

This thesis attempts to understand and test the trapezoidal dog clutch by using multibody simulation software.

For that, initially started to draw the geometry of the dog clutch in 3D modelling software and the main focus was required to be choose the angle of contact faces and chamfered front face. The minimum angle of the contact faces chose in the way to avoid the self-locking and maximum angle is resisted by the axial force generated by the dog clutch during the engagement. The face chamfered angle chosen to reduce the face friction phase especially at high relative angular velocity there would no face to face contact and it is reducing the gear shifting time.

In the lab Juliska experiment was conducted using MQ 200 FCU gearbox in inertia test bench. Each experiment date was analyzed to get more information like a maximum force timing, relative angular velocity and shift force at sleeve. These values are integrated with simulation to run a simulation as real as possible.

I created Multibody simulation model in the MSC ADAMS environment to simulating gear shift between neutral to 3rd gear. Then sensitivity analysis carried out for contact parameters like stiffness, damping, static and dynamic coefficients but due to some uncertainty's these values are taken from the previous research work. The ADAMS model was simulated to find the engagement time on account of its different relative angular velocity and shift force and the results were successful.

To verify the simulation result, it is compared with experimental results. The simulation average engagement time is less compared to the experimental result and in chapter 5. explained what possibility reason for this time difference are.



Nomenclature and abbreviations

ADAMS	Automated Dynamic Analysis of Mechanical Systems	-
DOF	Degrees of freedom	-
Z	overall clutch displacement	m
h	dog height	m
Z_{gap}	Clearance between two half clutches	m
ω_{rel}	Relative angular velocity	rad/sec
ω_1	Angular velocity of sliding dog	rad/sec
ω_2	Angular velocity of output dog	rad/sec
K	Stiffness coefficient	N/m
δ	Penetration depth	m
$\dot{\delta}$	Penetration depth velocity	m/s
e	Force exponent	-
d_{max}	Penetration depth at which maximum damping is applied	[m
C_{max}	Maximum damping coefficient	N-s/m
$\Phi(q)$	Constraint equation	-
q	Generalized coordinate system	-
T	Total kinetic energy	J
V	Potential energy	J
J	Inertia matrix	-
λ	Lagrange multiplier vector	-
Q	External force vector	N
m	Total number of constraints	-
n	Number of generalized coordinates	-



F_N	Normal contact force	N
F_t	Tangential friction force	N
V	Slip velocity at contact point	m/s
V_s	Stiction transition velocity	m/s
V_d	Friction transition velocity	m/s
μ_s	Static friction coefficient	-
μ_d	Dynamic friction coefficient	-
J_{red}	Reduced moment of inertia	Kg m ²
J_{out}	Output dog clutch moment of inertia	Kg m ²
i_3	Third gear ratio	-
i_{diff}	Differential gear ratio	-
α	Angle of dog side faces	deg
β	Chamfered face angle	deg
\vec{v}	Velocity vector [m/s]	[m/s
v_1, v_2	Velocity vector decomposition [m/s]	m/s
I_{xx}, I_{yy}, I_{zz}	principle moment of inertia [Kg m ²]	Kg m ²
G	Gravitational force [N]	N
m	Mass of the object [Kg]	Kg
g	Gravitational acceleration [m/s ²]	m/s ²
DOE	Design of Experiments [-]	-
x	Number of runs [-]	-
y	Number of parameters to change [-]	-
MBD	Multibody dynamics [-]	-
MBS	Multibody system [-]	-



<i>ODE</i>	Ordinary differential equation [-]	-
<i>DAE</i>	Differential algebraic equation [-]	-
<i>BDF</i>	Backward differential formula [-]	-
<i>GSTIFF</i>	Gear stiff Integrator [-]	-
<i>WSTIFF</i>	Modified Gear Integrator	-
<i>RKF45</i>	Runge-Kutta-Fehlberg method [-]	-
<i>ABAM</i>	Adams–Bashforth–Adams–Moulton [-]	-
<i>f(t)</i>	Exact solution	m
<i>p(t)</i>	Approximate solution	m



References

- [1] Gabriela Achtenová, Jiří Pakosta, "ResearchGate," Smoothness of Maybach dog clutch shift in the automotive gearbox, 2014.
Available: https://www.researchgate.net/publication/280384542_Smoothness_of_Maybach_dog_clutch_shift_in_the_automotive_gearbox".
- [2] Jae-Oh Han, Jae-Won Shin, Jae-Chang Kim and Se-Hoon Oh, "ResearchGate," Chung-ang University, "Design 2-Speed Transmission for Compact Electric Vehicle Using Dual Brake System"
Available: https://www.researchgate.net/publication/332737685_Design_2-Speed_Transmission_for_Compact_Electric_Vehicle_Using_Dual_Brake_System
.
- [3] H. Naunheimer, Automotive Transmissions, Springer , 1994.
- [4] Motorcycle Gearbox,
[Online]. Available: <http://www.rrrtoolsolutions.com/articles/motorcycle-transmission-how-and-why-it-works/>.
- [5] Manual Transmission, "Wikipedia,"
[Online]. Available: https://en.wikipedia.org/wiki/Manual_transmission.
- [6] Matlab. Dog clutch simulation
[Online]. Available:
<https://www.mathworks.com/help/physmod/sdl/ref/dogclutch.html>.
- [7] Alexander F. Andreev, Viachaslau Kabanau, and Vladimir Vantsevich,
Driveline Systems of Ground Vehicles: Theory and Design, 2010.
- [8] Takashi Iwata, Kyosuke Mori, Taketoki Maruyama, Shinobu Nakamura, "SAE Mobilus,"
[Online]. Available: <https://saemobilus.sae.org/content/2016-01-1172>.
- [9] Trencsényi, Gergely Bóka / János Márialigeti / László Lovas / Balázs, periodica polytechnica, " Face dog clutch engagement at low mismatch speed"
[Online]. Available:
https://www.researchgate.net/publication/272869976_Face_dog_clutch_engagement_at_low_mismatch_speed.



- [10] Lipčák, Bc. Dmitrij, "Adaptation of internal shift mechanism for future automation," 2016.
- [11] Gabriela Achtenova, Michal Jasny, and Jiri Pakosta, "SAE Mobilus," 03 04 2018.
" Dog Clutch Without Circular Backlash "
[Online]. Available: <https://saemobilus.sae.org/content/2018-01-1299/>.
- [12] Achtenova, G. and Pakosta, J, Estimation of the Gearbox No-Load Losses, 04 05 2016.
[Online]. Available: <https://saemobilus.sae.org/content/2016-01-1092/>.
- [13] Solver, ADAMS, "MSC ADAMS," 2011.
[Online]. Available:
https://simcompanion.mscsoftware.com/infocenter/index?page=content&id=DOC10102&cat=2011_A30&actp=LIST&showDraft=false.
- [14] Song, Peng, 2002. " Modeling, Analysis and Simulation of multibody systems with contact and friction "
[Online]. Available: <ftp://ftp.cis.upenn.edu/pub/kumar/thesis/pengs.pdf>.
- [15] Lagrangian mechanics, "wikipedia,"
[Online]. Available: https://en.wikipedia.org/wiki/Lagrangian_mechanics.
- [16] Fan Luo, Jinning Li, Xingxing Feng, Yunqing Zhang,
[Online]. Available: <https://saemobilus.sae.org/content/2015-01-0633>.
- [17] Giesbers, Jochem, 11 July 2012.
[Online]. Available: https://essay.utwente.nl/62109/1/BSc_J_Giesbers.pdf.
- [18] ADAMS, Contact , "ADAMS help manual".
- [19] ADAMS, "Contact friction force calculation".
- [20] Self-lock. [Online]. Available: <https://www.motioncontroltips.com/when-are-worm-gears-self-locking-and-where-is-this-useful/>.
- [21] Steel alloy Material property, [Online]. Available:
<https://steelnavigator.ovako.com/steel-grades/16mncr5/?acceptCookies=true>.



List of Figures

<i>Figure 1 - Comparison of dog clutch and synchronizer [1, p. 3]</i>	<i>2</i>
<i>Figure 2 - 2 speed gearboxes with dog clutch [3, pp. 15, 301]</i>	<i>5</i>
<i>Figure 3 - Motorcycle gearbox [4]</i>	<i>6</i>
<i>Figure 4 - Dog clutch overall displacement [6]</i>	<i>7</i>
<i>Figure 5 - Permanent face to face contact</i>	<i>8</i>
<i>Figure 6 - Bounce-back effect [8, p. 4]</i>	<i>9</i>
<i>Figure 7 - Engagement process of dog clutch [9, p. 2]</i>	<i>10</i>
<i>Figure 8 - Dog clutch initial contact position</i>	<i>11</i>
<i>Figure 9 - Dog design according to the insertion slope</i>	<i>13</i>
<i>Figure 10 - Input and output shaft of the passenger car gear-box with Maybach dog clutch between the 3rd and 4th speed [1, p. 4]</i>	<i>14</i>
<i>Figure 11- Exploded view of Pakoshift clutch</i>	<i>15</i>
<i>Figure 12 - Shift Sequence of Pakoshift [10, p. 36]</i>	<i>16</i>
<i>Figure 13 - Exploded view of Dog clutch with blocking mechanism</i>	<i>17</i>
<i>Figure 14 - Dog clutch at neutral position [12, p. 4]</i>	<i>18</i>
<i>Figure 15 - Scheme of the inertia test stand.</i>	<i>20</i>
<i>Figure 16 - Flywheel inertia test bench</i>	<i>21</i>
<i>Figure 17 - Global coordinate system and Local coordinate system [13, p. 39]</i>	<i>24</i>
<i>Figure 18 - Dog to Dog contact dynamics</i>	<i>29</i>
<i>Figure 19 - Shows the behavior of the IMPACT function's spring force and damping force [17, p. 12]</i>	<i>30</i>
<i>Figure 20 - Damping coefficient vs Penetration [18]</i>	<i>31</i>
<i>Figure 21- Coefficient of friction Vs slip velocity [19]</i>	<i>32</i>



Figure 22 - Test bench measurement with relative angular speed difference of 49.8 rpm	33
Figure 23 - Linkage ratio.....	35
Figure 24 - (a) Incorrect and (b) correct geometry of trapezoidal dog [7, pp. 247-248]	39
Figure 25 – Geometry of trapezoidal dog.....	40
Figure 26 - Velocity vector at dog	41
Figure 27 – Scheme of dog clutch in ADAMS.....	43
Figure 28 - Gearshift force at $\Delta\omega = 100$ rpm, $F_{max}=469$ N	44
Figure 29 - Normal contact force and tangential friction force	45
Figure 30 - DOE result for Stiffness and Damping compared with experiment	47
Figure 31 - Simulation measurement with $\Delta\omega =24.9$ rpm, sliding dog angle $=37^0$ and $F = 235$ N	50
Figure 32 - Average engagement time $F=469$ N, $\Delta\omega \neq$ constant.....	52
Figure 33 - Displacement of robot arm and simulation	53
Figure 34 - Average engagement time $\Delta\omega=100$ rpm, $F\neq$ constant	54
Figure 35 - Average engagement time $F=235.2$ N, $\Delta\omega \neq$ constant	67
Figure 36 - Average engagement time $F=315.5$ N, $\Delta\omega \neq$ constant	67
Figure 37 - Average engagement time $F=641.5$ N, $\Delta\omega \neq$ constant	68
Figure 38 - Average engagement time $\Delta\omega=10$ rpm, $F\neq$ constant.....	68
Figure 39 - Average engagement time $\Delta\omega=25$ rpm, $F\neq$ constant.....	69
Figure 40 - Average engagement time $\Delta\omega=50$ rpm, $F\neq$ constant.....	69
Figure 41 - Average engagement time $\Delta\omega=249$ rpm, $F\neq$ constant	70
Figure 42 - Average engagement time $\Delta\omega=149$ rpm, $F\neq$ constant	70
Figure 43 - DOE results for stiction and dynamic transition velocity and $\Delta\omega = 100$ rpm	71



Figure 44 - DOS for $V_s = 1E-3$ m/s, $V_d = 1E-2$ m/s and $\Delta\omega \neq \text{constant}$ 71

Figure 45 - DOS for $V_s = 0.1$ m/s, $V_d = 1$ m/s and $\Delta\omega \neq \text{constant}$ 72

Figure 46 - Trapezoidal dog drawing using CATIA V5 73



List of Tables

<i>Table 1 - Gear ratio of tested gearbox.....</i>	<i>20</i>
<i>Table 2 - Gearshift force at sleeve</i>	<i>36</i>
<i>Table 3 - Relative angular velocity (rpm).....</i>	<i>37</i>
<i>Table 4 - Average engagement time in experiment.....</i>	<i>37</i>
<i>Table 5 - Dog design parameters.....</i>	<i>40</i>
<i>Table 6 - Mass and Principle mass moment of inertia.....</i>	<i>43</i>
<i>Table 7 - Contact force parameter used for simulation.....</i>	<i>48</i>
<i>Table 8 - Friction force parameter used for simulation</i>	<i>48</i>
<i>Table 9 - ADAMS used Solver parameters</i>	<i>50</i>
<i>Table 10 - Average engagement time in simulation.....</i>	<i>51</i>



List of attachments

- CAD models using CATIA software
- Experimental data analysis file using MS Excel
- Simulation models using MSC ADAMS



Appendix

Validation results

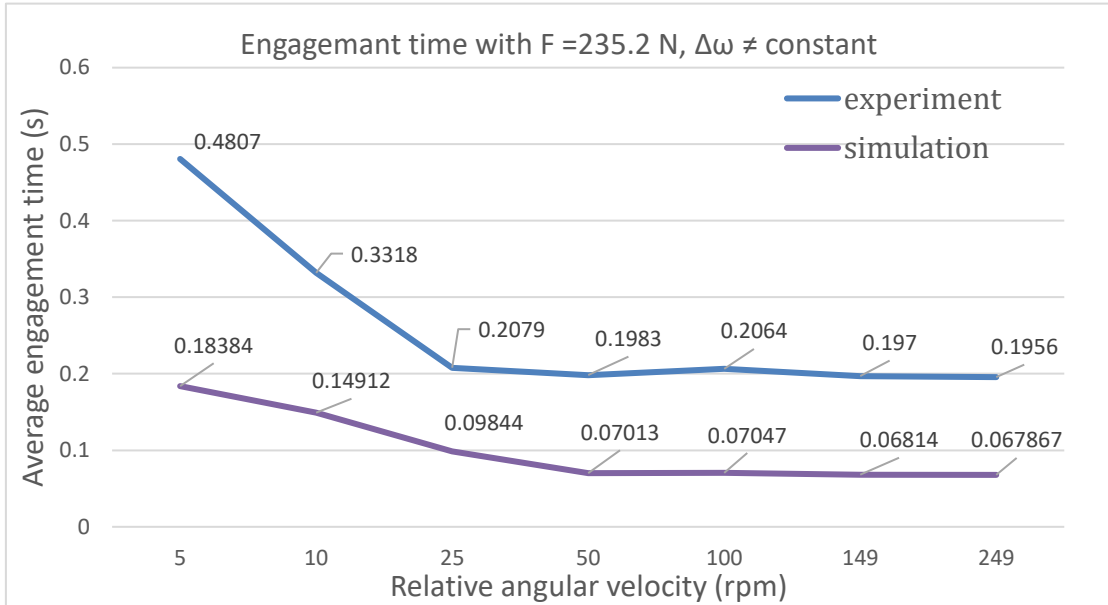


Figure 35 - Average engagement time $F=235.2 \text{ N}$, $\Delta\omega \neq \text{constant}$

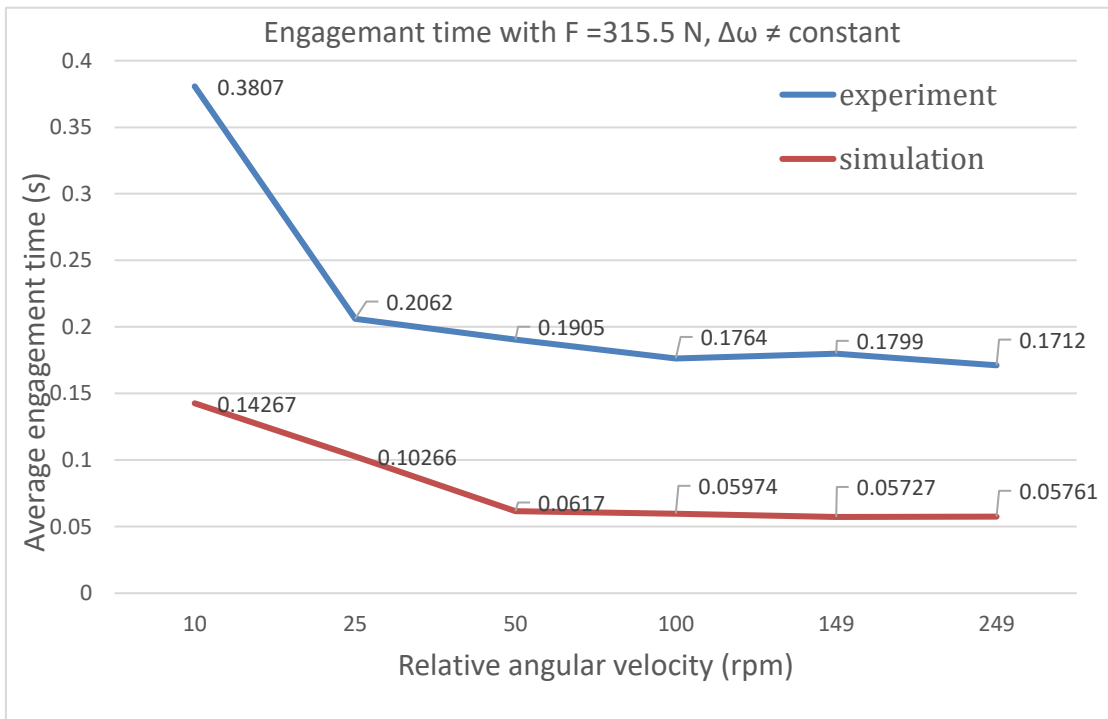


Figure 36 - Average engagement time $F=315.5 \text{ N}$, $\Delta\omega \neq \text{constant}$

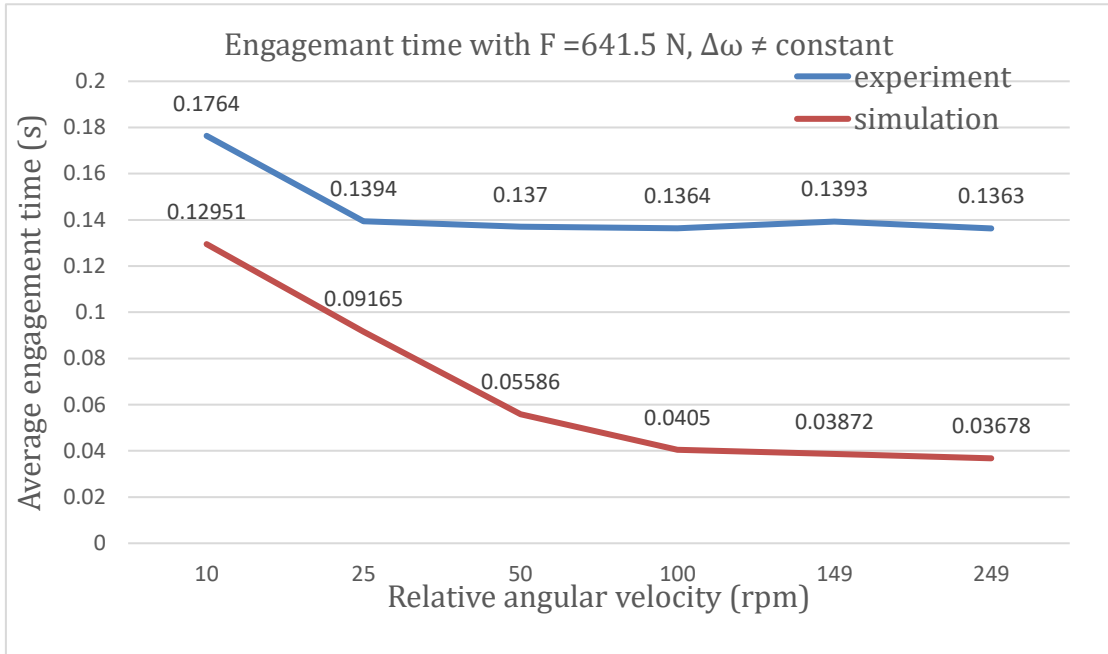


Figure 37 - Average engagement time $F=641.5 \text{ N}$, $\Delta\omega \neq \text{constant}$

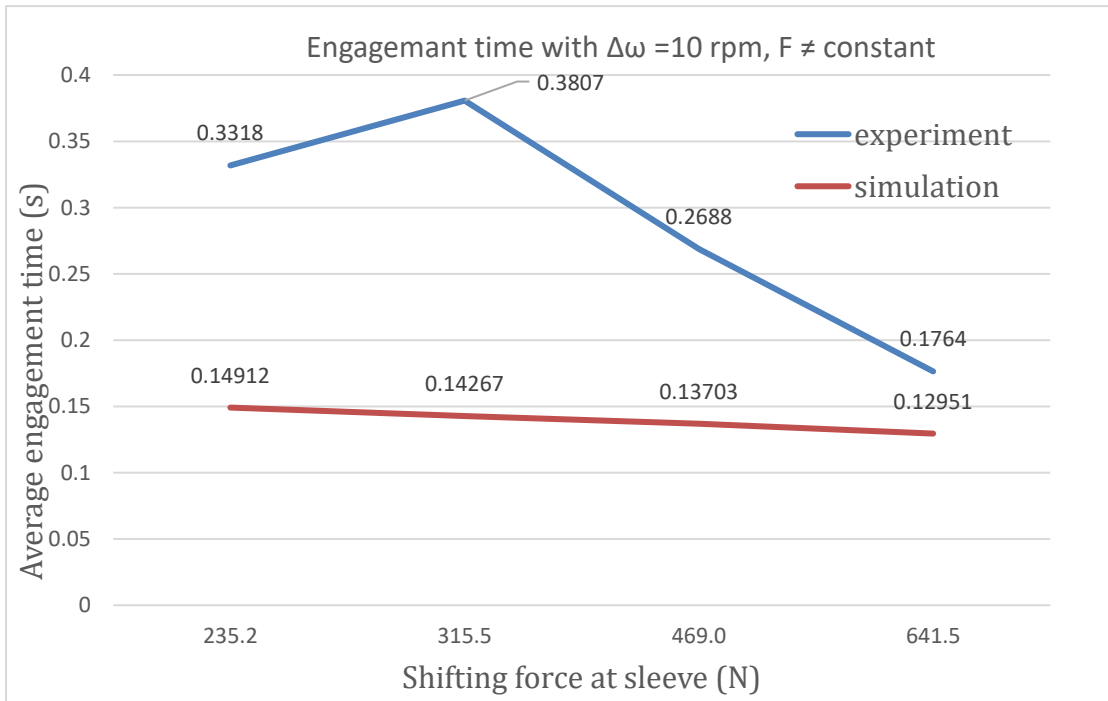


Figure 38 - Average engagement time $\Delta\omega=10 \text{ rpm}$, $F \neq \text{constant}$

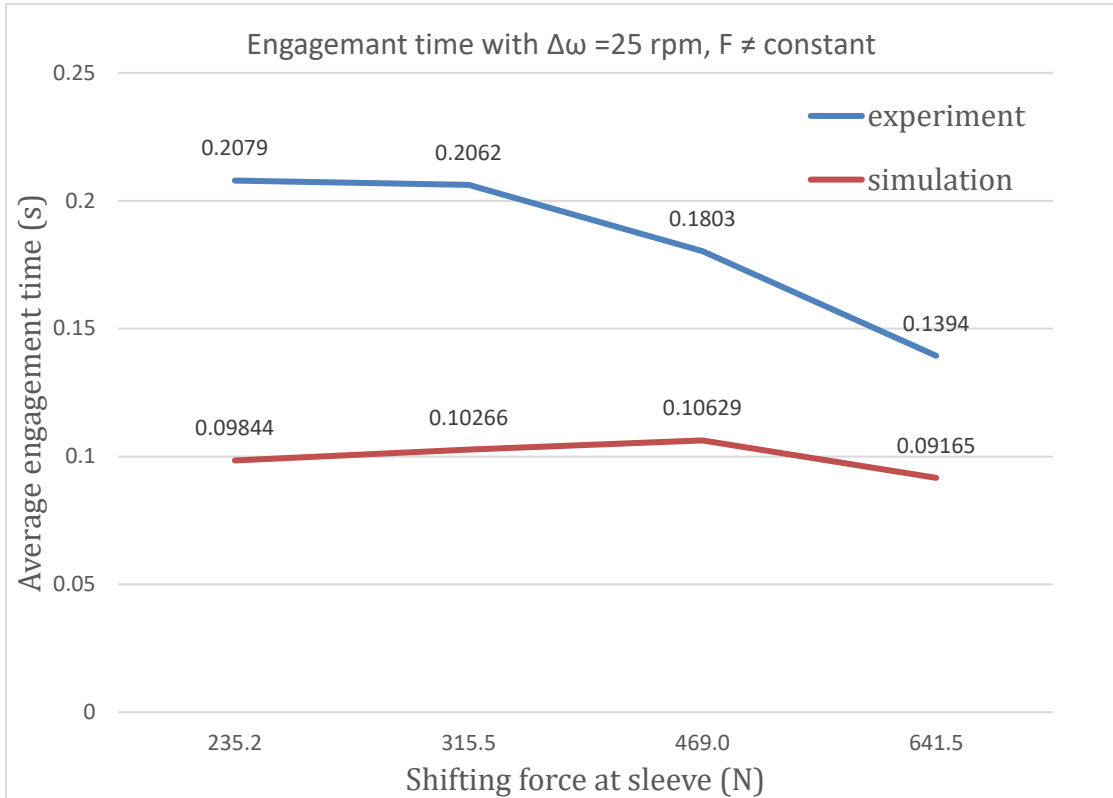


Figure 39 - Average engagement time $\Delta\omega=25$ rpm, $F \neq$ constant

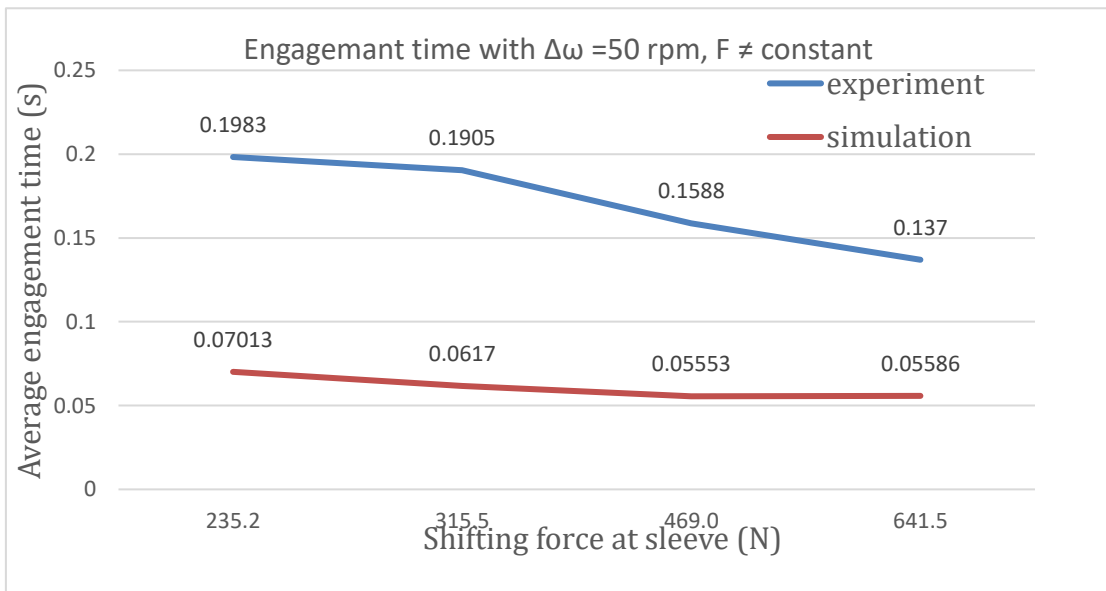


Figure 40 - Average engagement time $\Delta\omega=50$ rpm, $F \neq$ constant

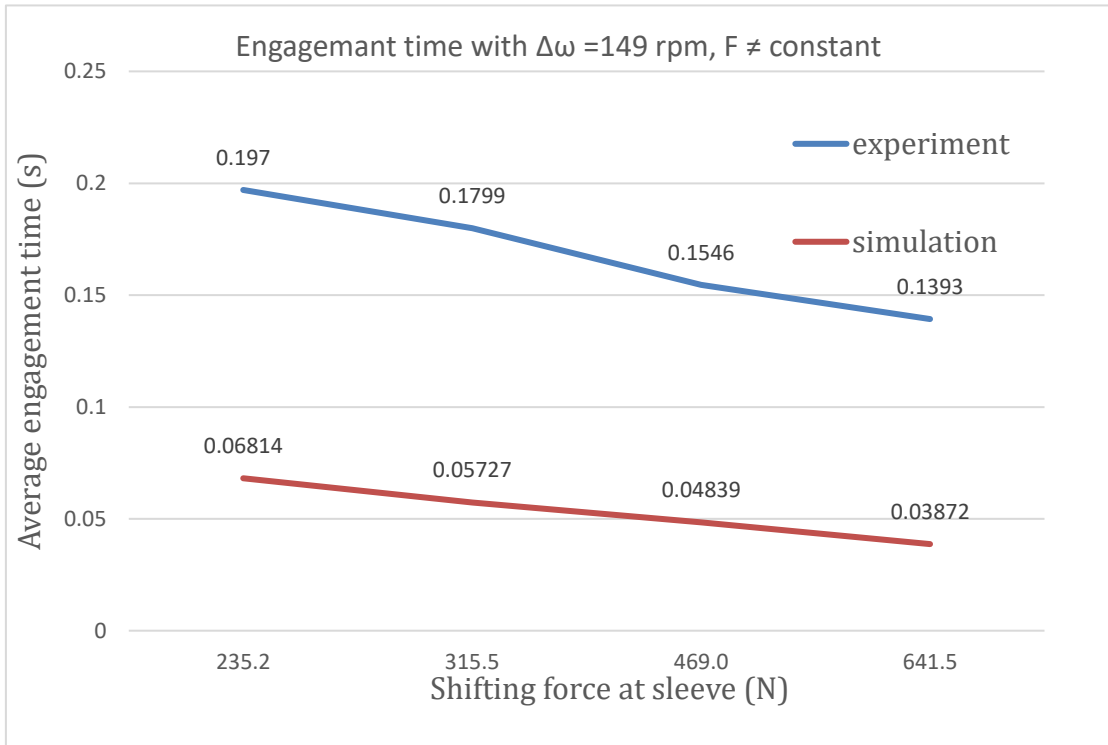


Figure 42 - Average engagement time $\Delta\omega=149$ rpm, $F \neq$ constant

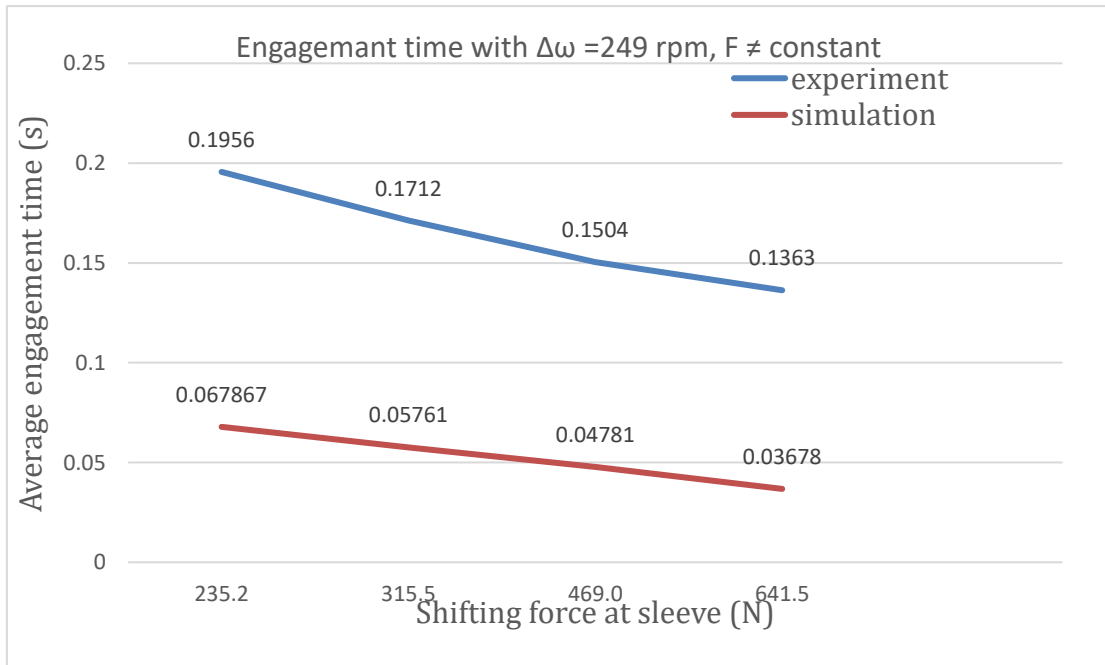


Figure 41 - Average engagement time $\Delta\omega=249$ rpm, $F \neq$ constant



Design of Experiment results

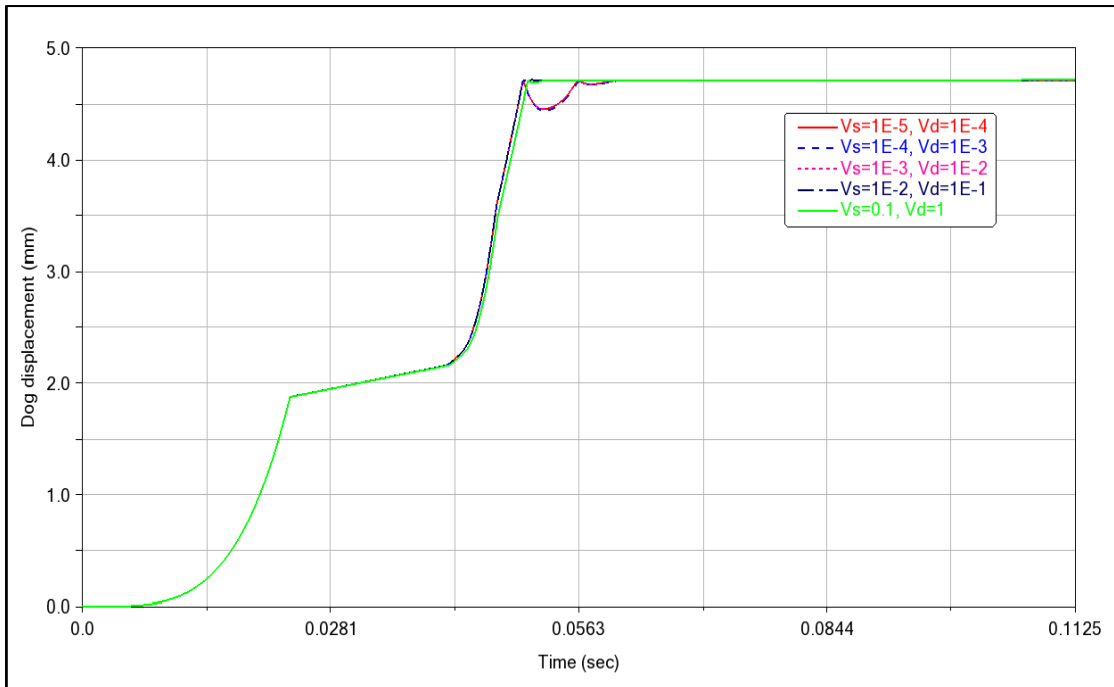


Figure 43 - DOE results for stiction and dynamic transition velocity and $\Delta\omega = 100$ rpm

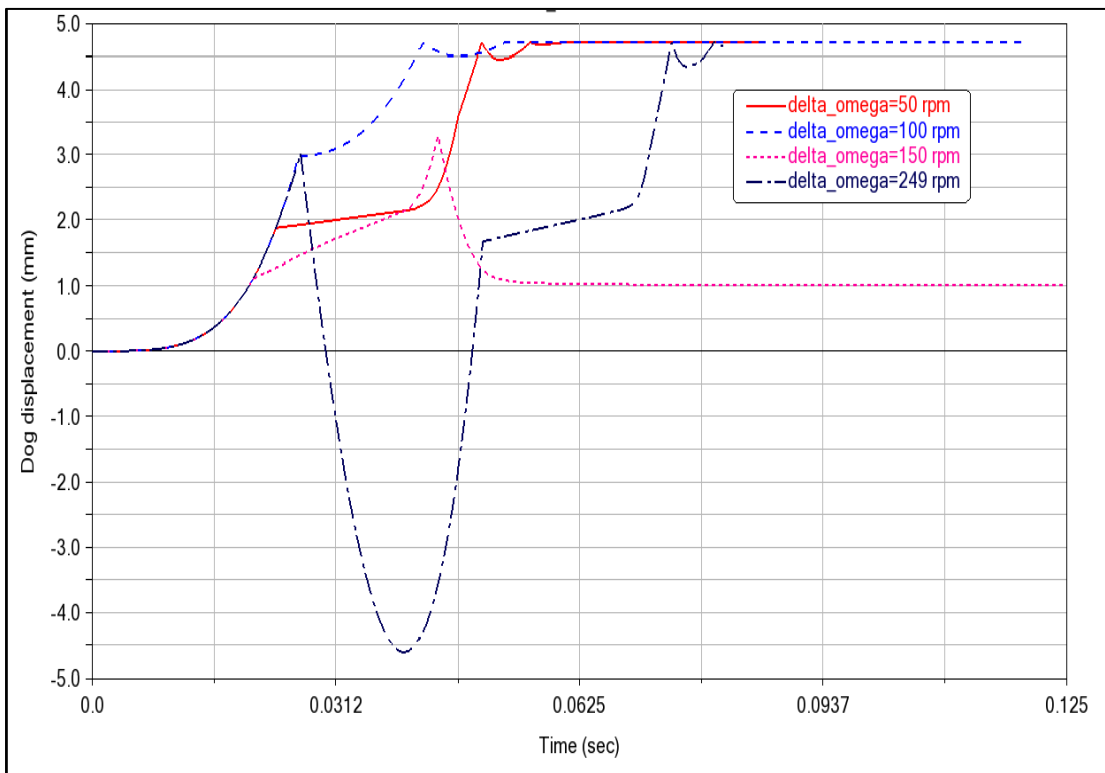


Figure 44 - DOS for $V_s = 1E-3$ m/s, $V_d = 1E-2$ m/s and $\Delta\omega \neq$ constant

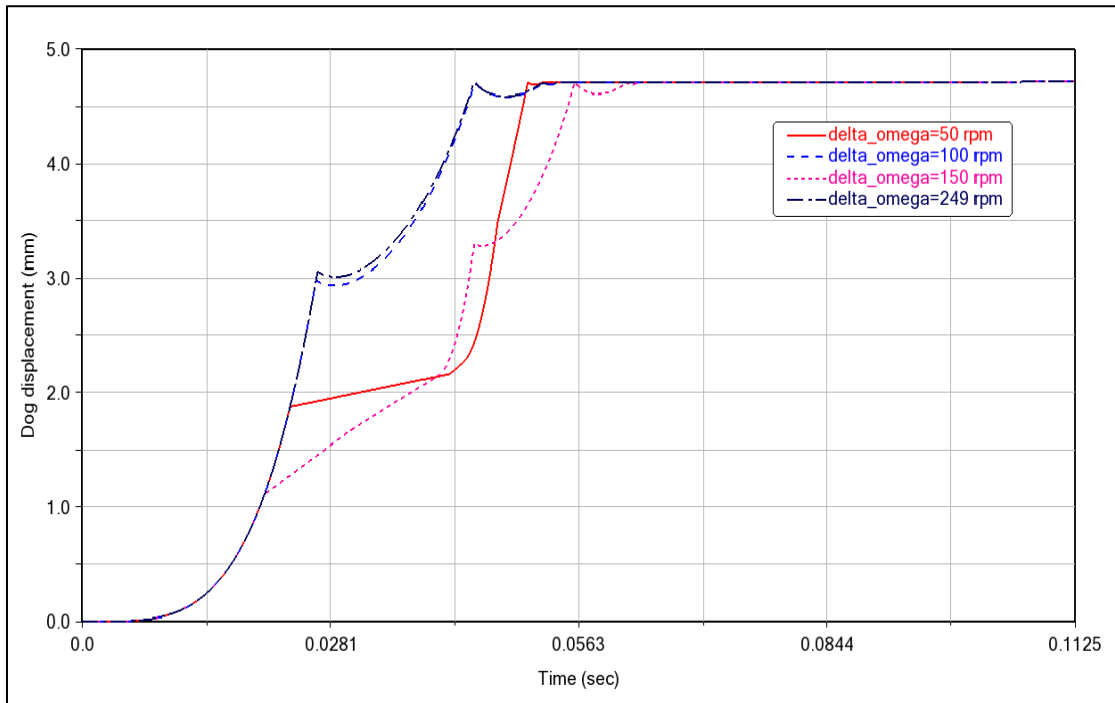


Figure 45 - DOS for $V_s = 0.1$ m/s, $V_d = 1$ m/s and $\Delta\omega \neq \text{constant}$

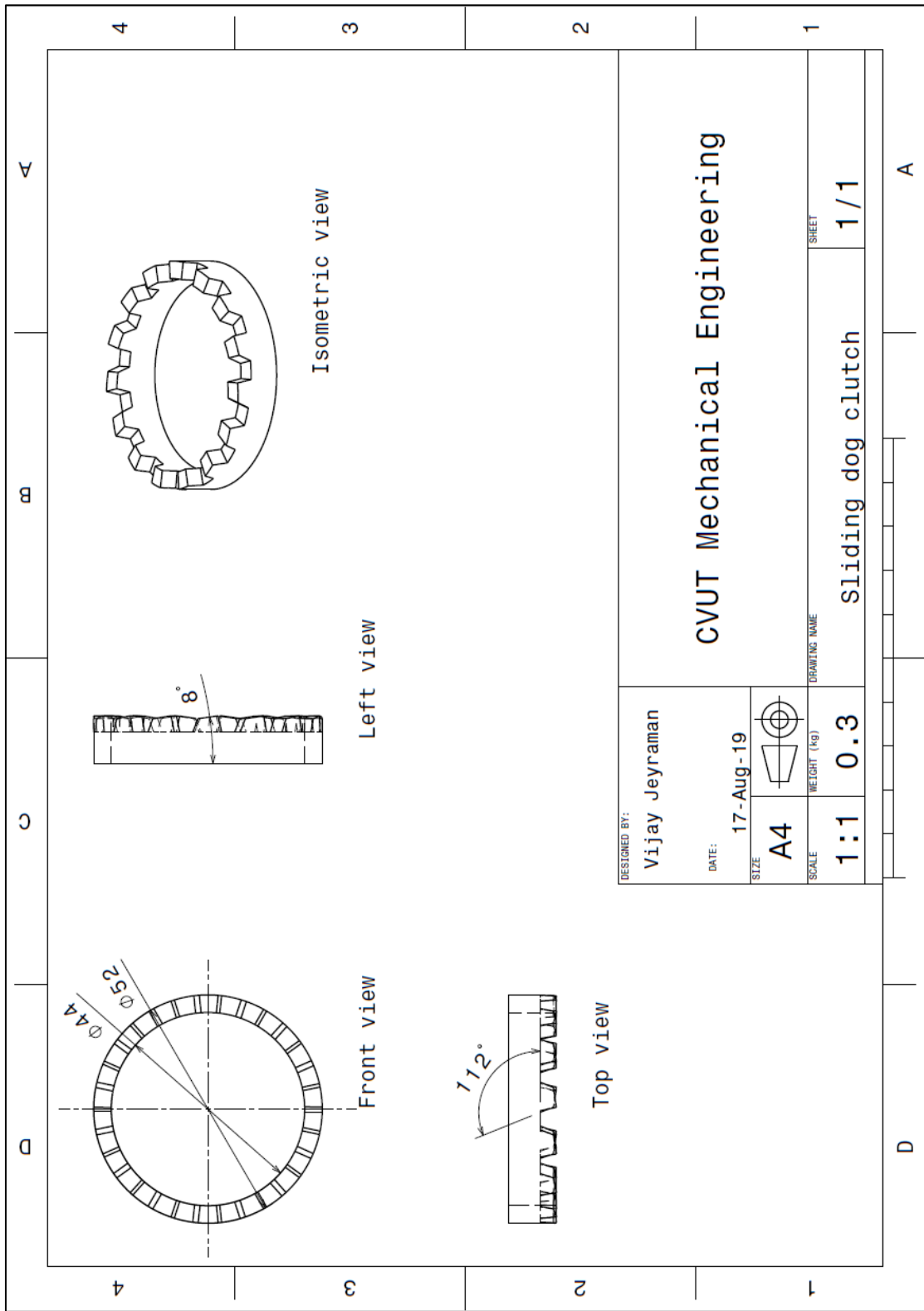


Figure 46 - Trapezoidal dog drawing using CATIA V5